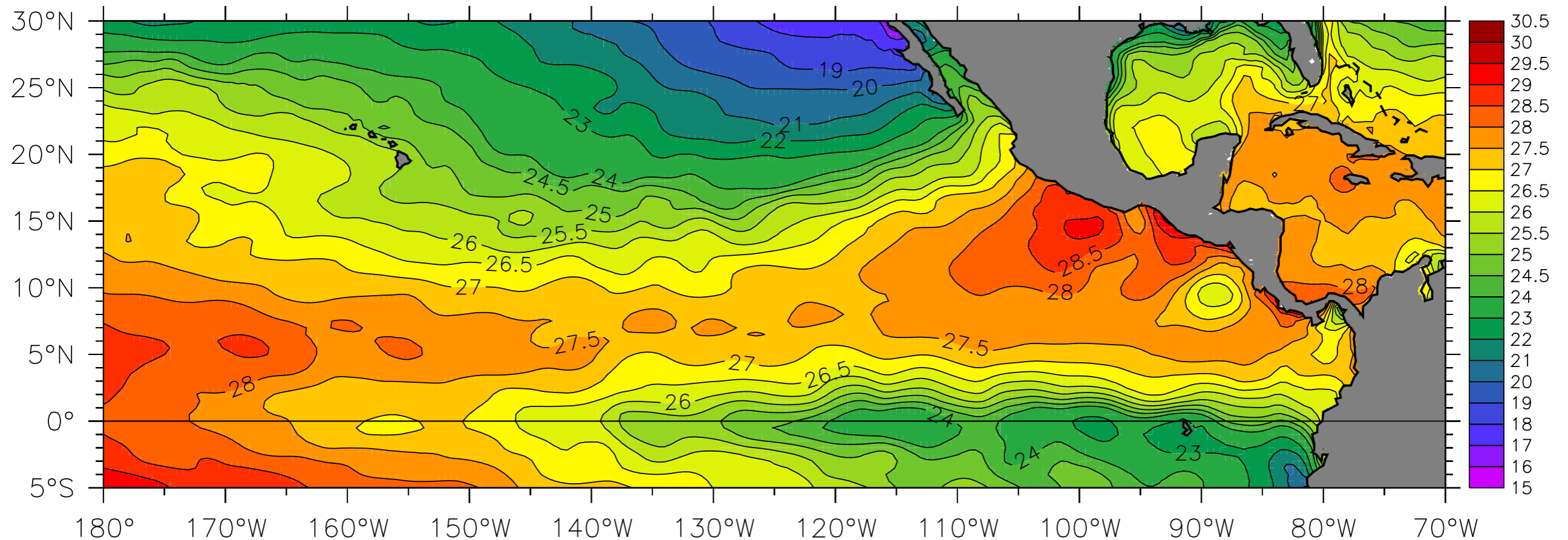


Ocean dynamics of the East Pacific Warm Pool and its consequences

Mean SST (CARS)



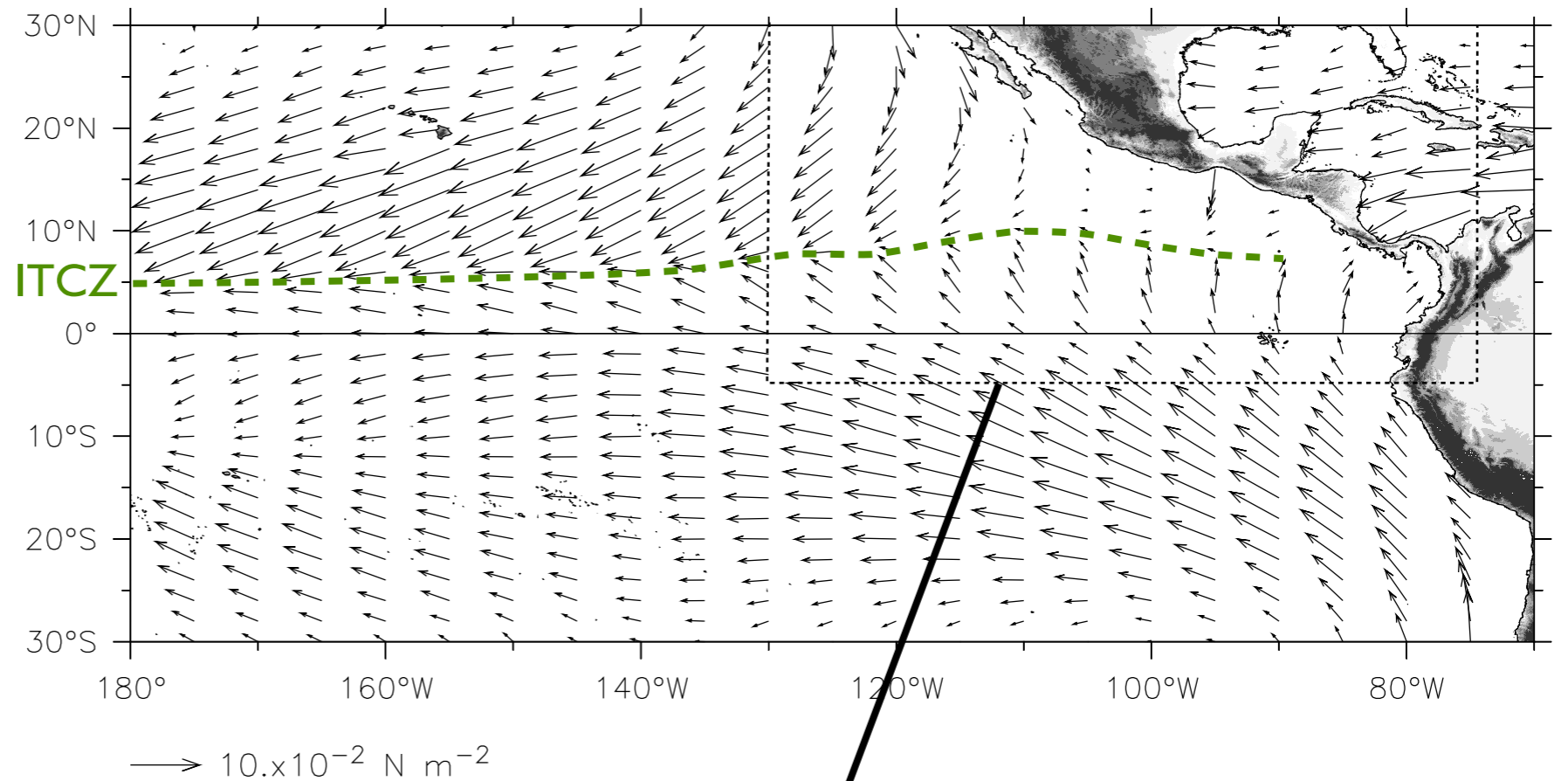
William S. (Billy) Kessler
NOAA / PMEL
Seattle USA

La Paz, B.C.Sur, Mexico. March 2013

Outline

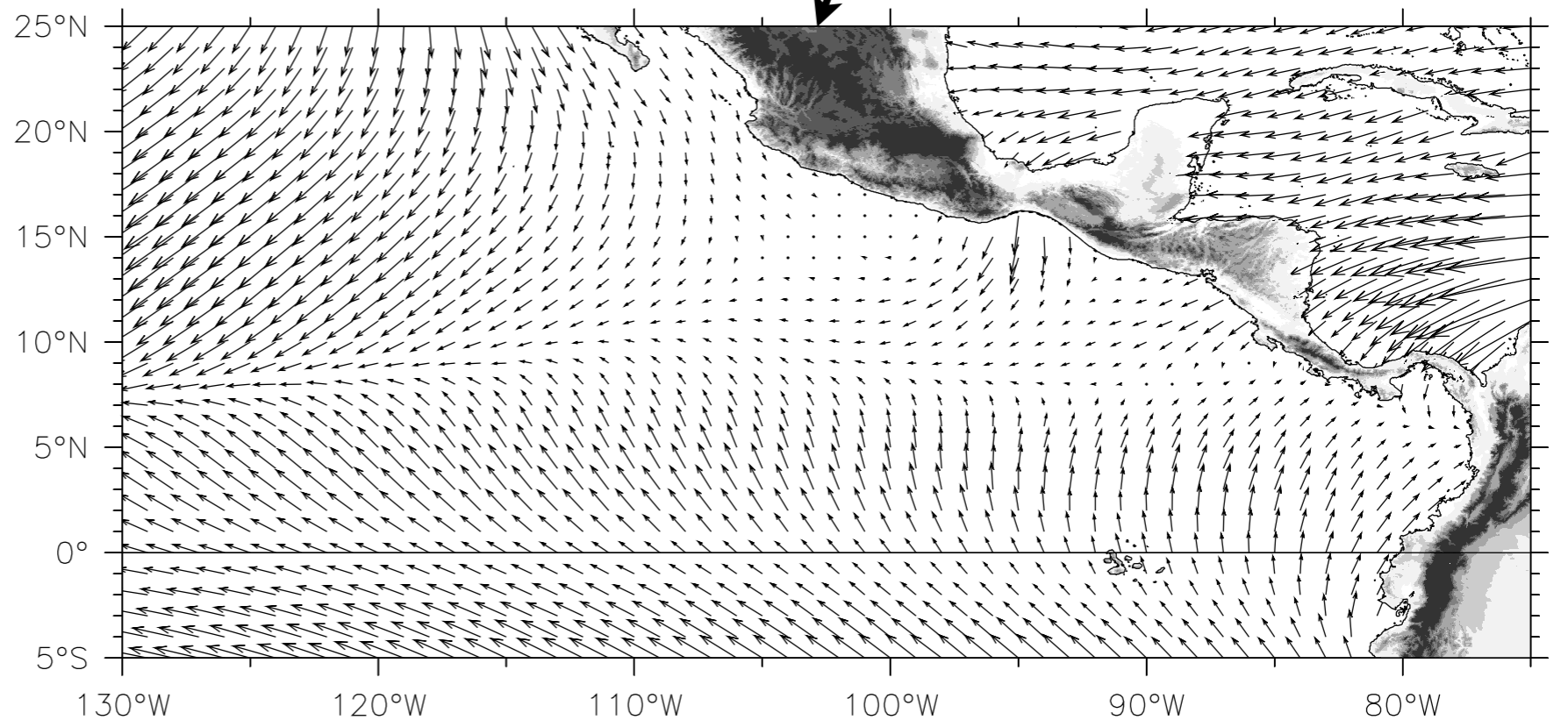
- What's special about the East Pacific Warm Pool?
- Role of wind-driven linear ocean dynamics
... and what it doesn't explain.
... forces determining the “shape” of the NE tropical Pacific
- Processes: linear and non-linear (anticyclonic eddies)
- How the Costa Rica Dome influences the general circulation of the Pacific.
- Feedbacks to the atmosphere

Central Pacific winds
are uniform in x
long zonal scales: $d/dx \sim 0$



Weaker mean winds
over EPWP
Significant zonal gradients,
short zonal scales

Caribbean trades impinge
on Central America: blow
through gaps



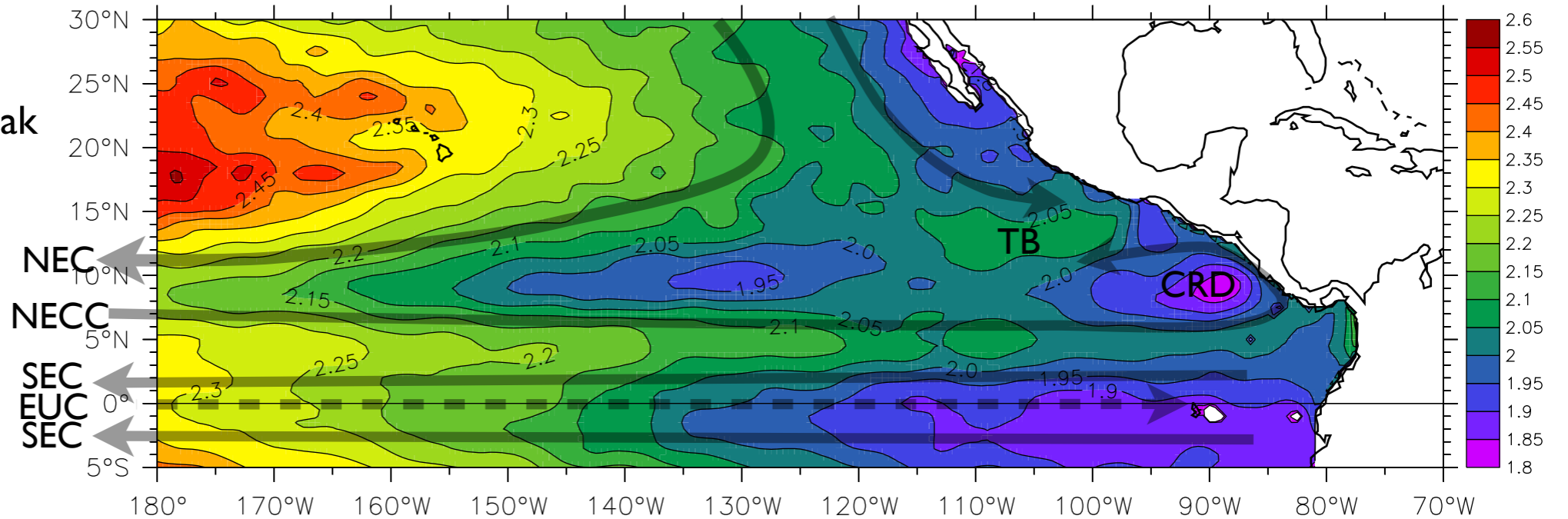
Large-scale circulation

Upper currents

The ridges and troughs of the central Pacific break up in the east.

An oceanic description of the NETP is where the N. Pacific gyre does not reach into the large bight from Mexico to Ecuador.

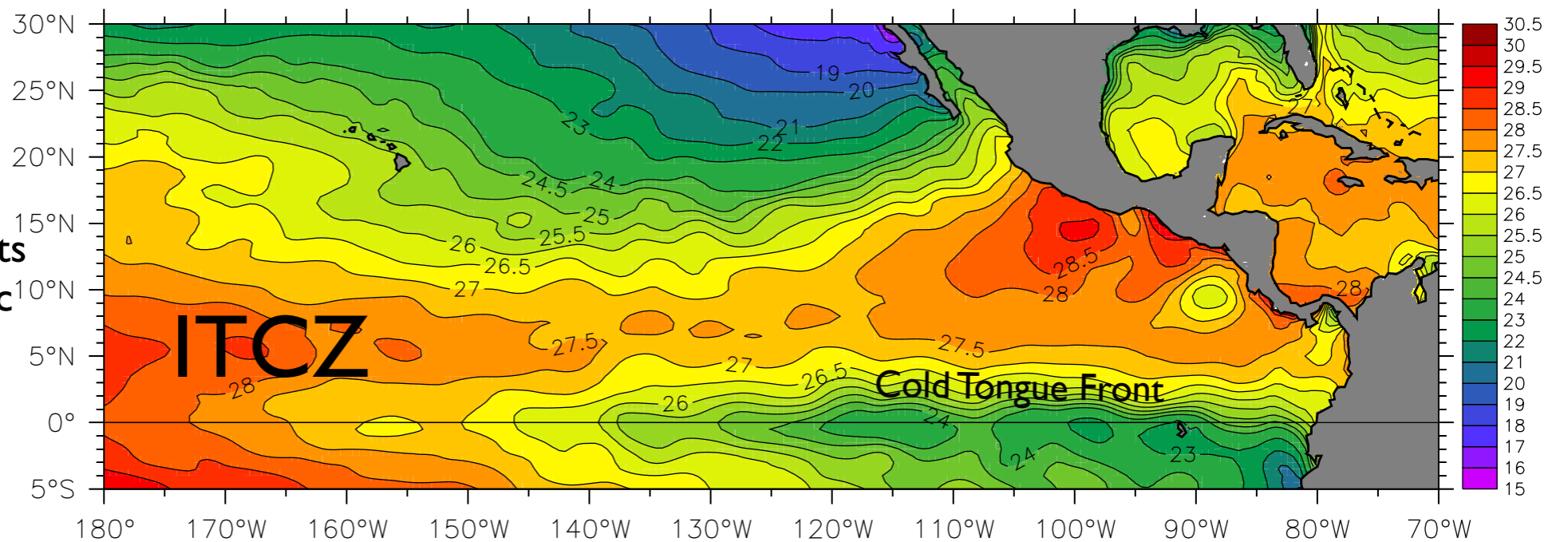
Dynamic height relative to 2000m



East Pacific Warm Pool

Although the NECC connects the NETP to the West Pacific Warm Pool, advection does not account for its high SST.

Mean SST



Circulation from surface drifters

(Blanks = no sampling)

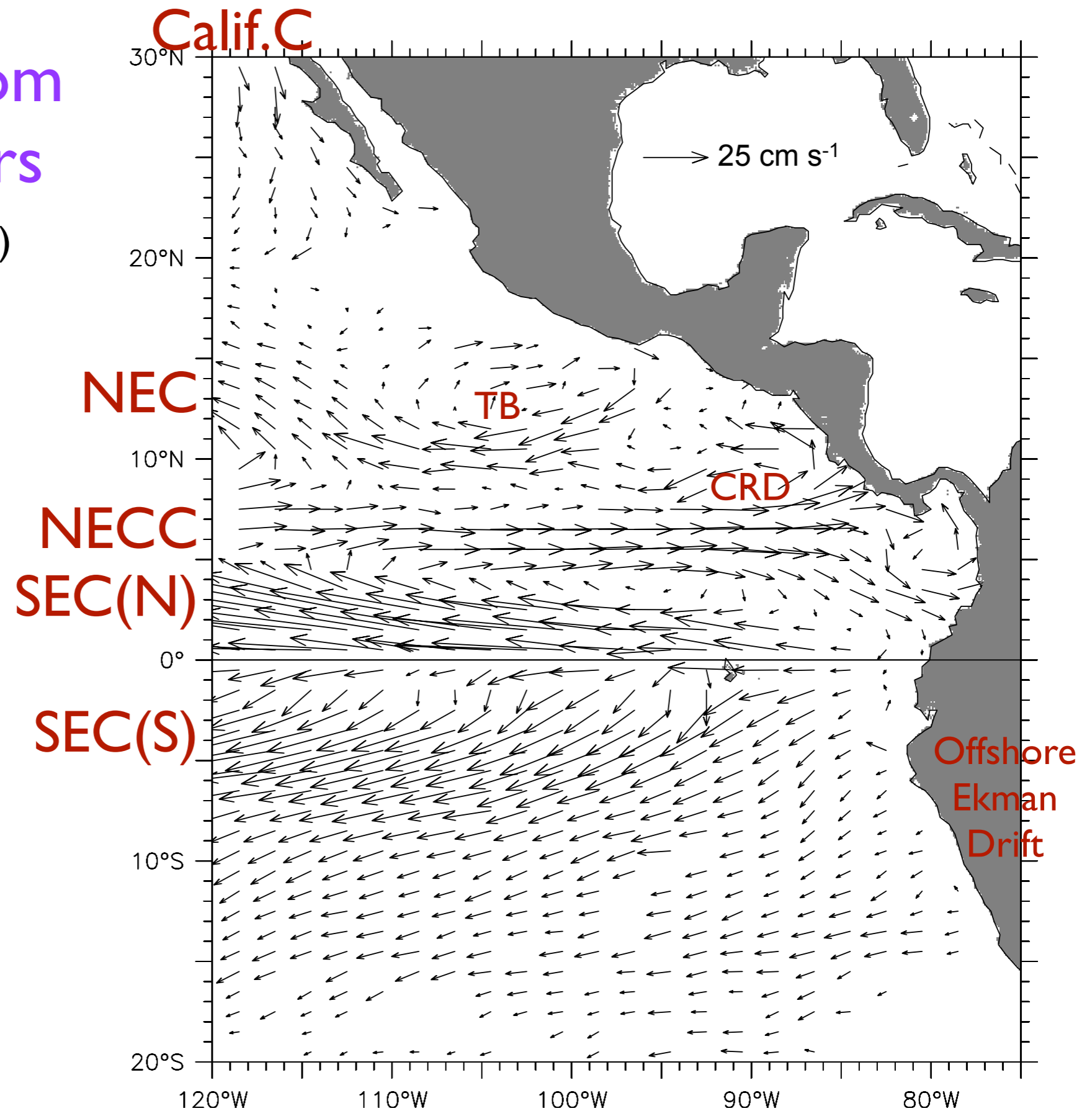


Fig. 4. Mean surface circulation from surface drifters. Vectors were left blank if either the total count of samples in that 1° × 1° box was less than 10, or if fewer than 4 months of the year were represented. The scale vector is located in the Gulf of Mexico.

Winds and Curl(τ) over the EPWP

Dominated by gap jets: Tehuantepec, Papagayo, Panama

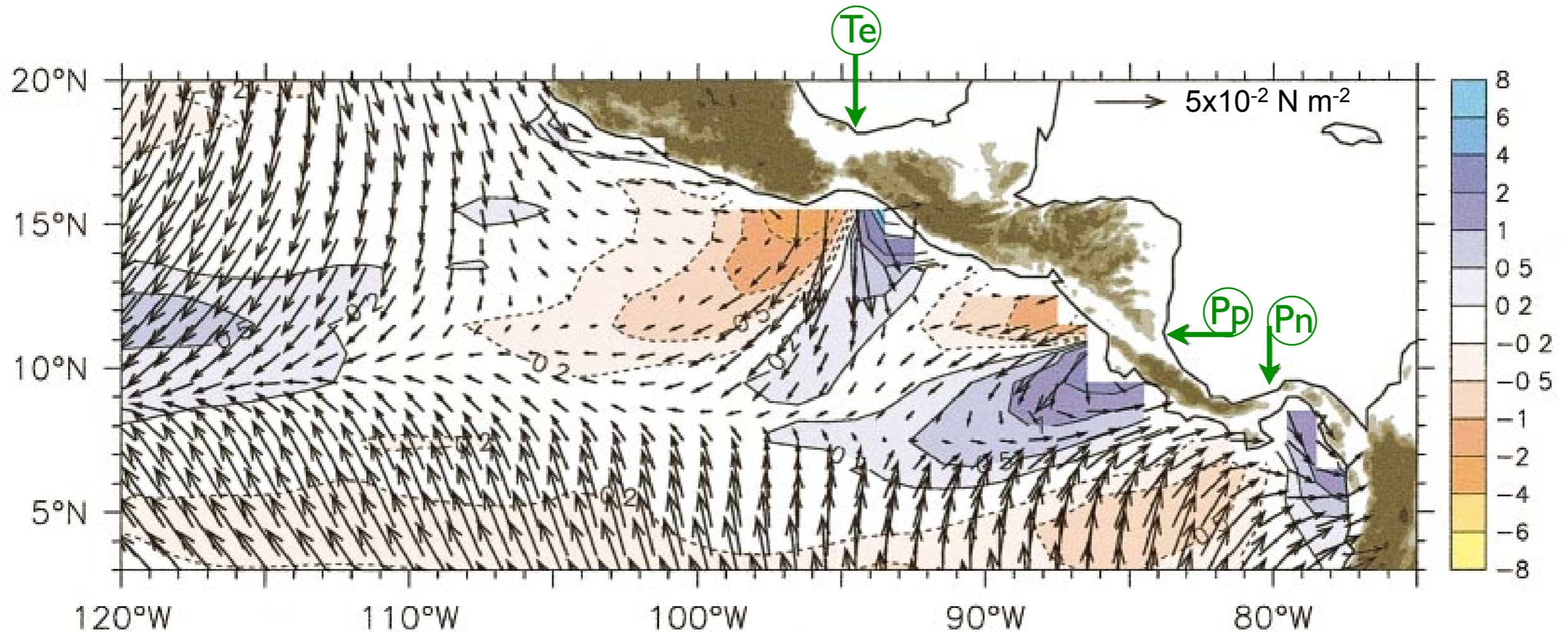
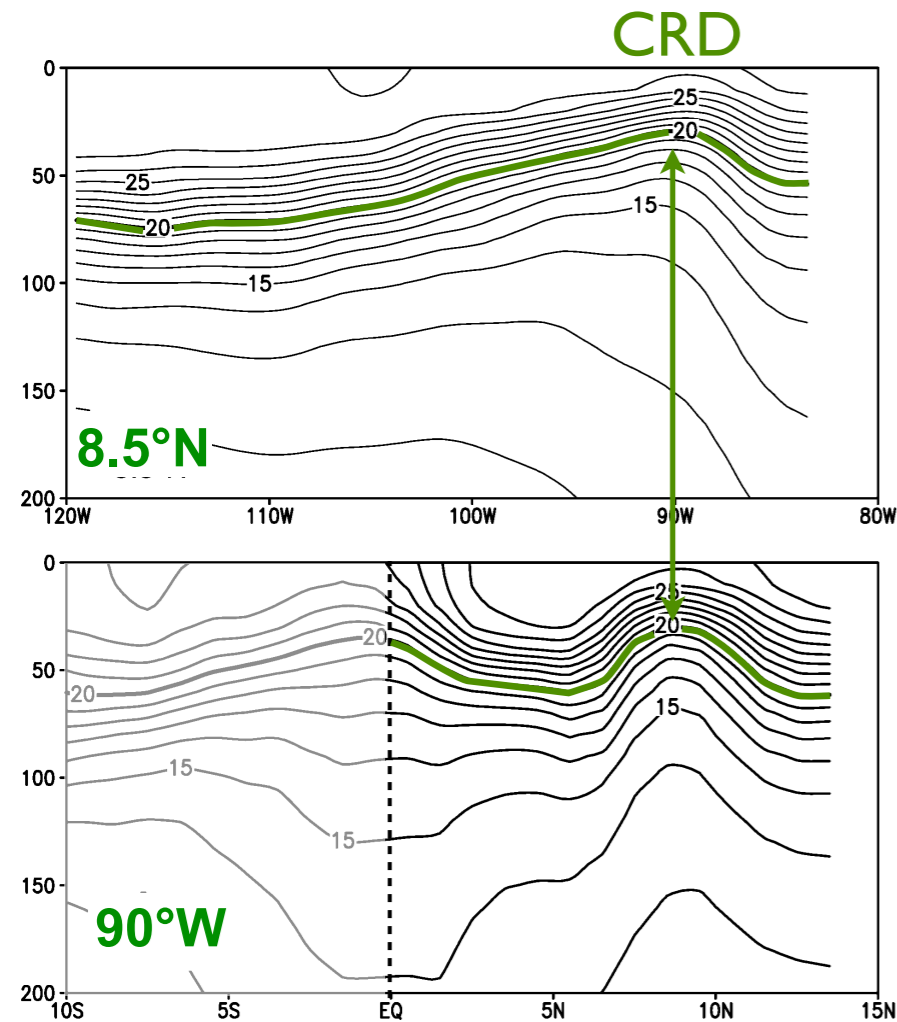


FIG. 5. Mean wind stress vectors and curl (colors) averaged over Aug 1999–Jul 2000. Red shading shows negative (downwelling) curl and blue positive (upwelling) curl, in units of 10^{-7} N m^{-3} , with (stretched) color key at right. The scale vector ($5 \times 10^{-2} \text{ N m}^{-2}$) is located in the Caribbean. The gray shading on land indicates altitudes greater than 250 m. The three mountain gaps referred to in the text are marked with arrows on the Caribbean side; from north to south these are denoted the Isthmus of Tehuantepec, the Gulf of Papagayo, and the Gulf of Panama.

NETP largely driven by wind forcing (unlike WPWP, Equator)

SST not a mirror of thermocline: Except Costa Rica Dome

Temperature cross-sections



Z20=Depth of the 20°C isotherm

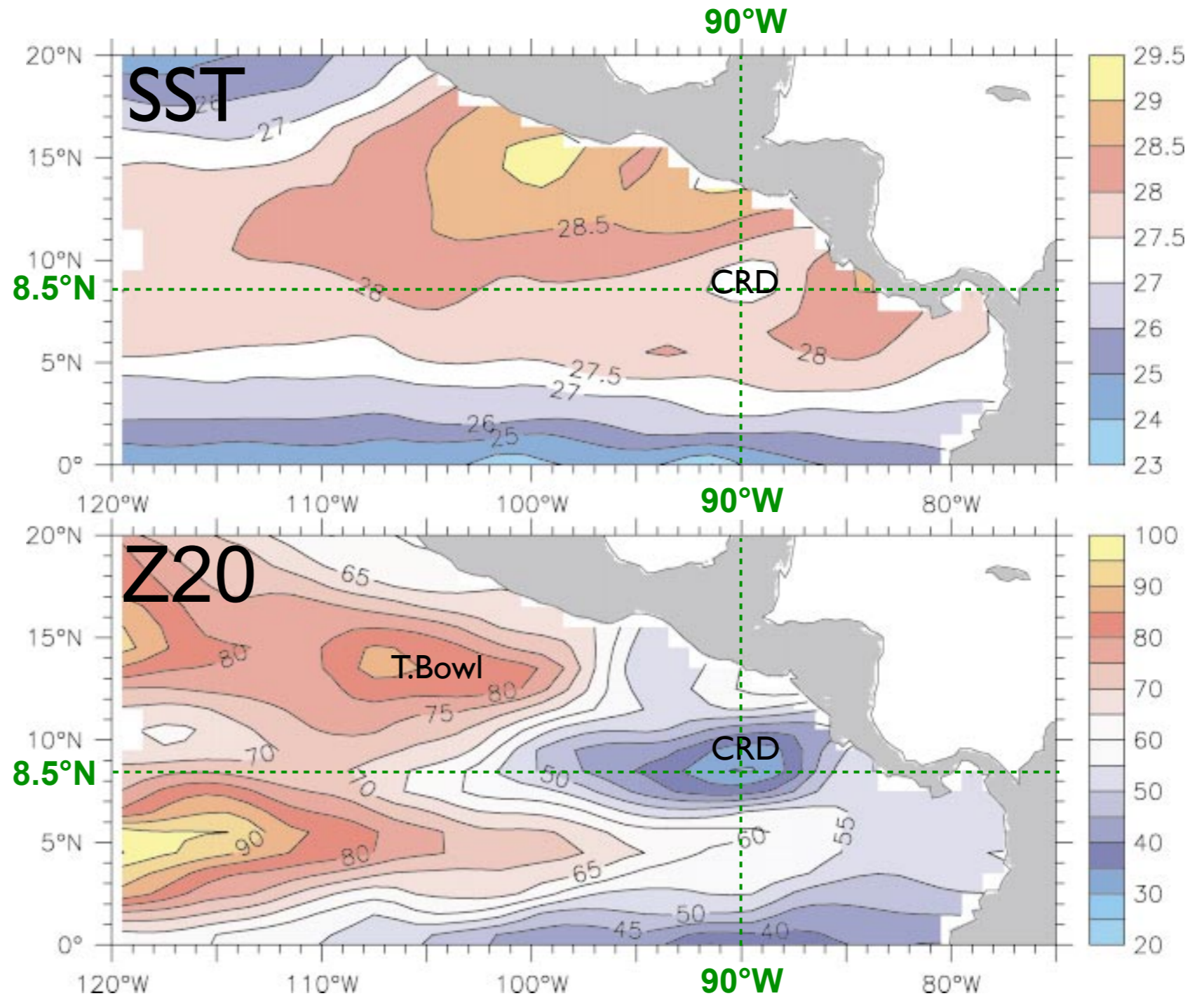


FIG. 2. Mean SST (top) and 20°C isotherm depth (Z20; bottom) from the XBT data. The contour interval for SST is 1°C, with supplementary contours at 27.5° and 28.5°C. Red shading indicates warm SST, blue cool. The contour interval for Z20 is 5 m. Red shading indicates deep thermocline; blue, shallow.

Why does the thermocline have this peculiar shape?

Linear, inviscid equations

A simplified ocean has a single active upper layer of mean depth H , overlying a deep, motionless abyss (not a bad assumption in the tropics where the thermocline is sharp).

Ignoring nonlinear and frictional effects (beyond the direct effect of the wind stress), the equations of motion and continuity can be written:

$$\begin{array}{cccc} \underline{\text{Time}} & \underline{\text{Coriolis}} & \underline{\text{Press. Grad}} & \underline{\text{Wind}} \\ u_t - fv & = & -g'h_x + \tau^x / \rho_0 H & \quad (1) \end{array}$$

$$v_t + fu = -g'h_y + \tau^y / \rho_0 H \quad (2)$$

$$h_t + H(u_x + v_y) = 0 \quad (3)$$

where

- (u, v) is the horizontal velocity,
- f is the Coriolis parameter (local vertical component of the earth's rotation),
- $h(x, y, t)$ is the upper layer thickness anomaly (positive down, and assuming $h \ll H$),
- $g' = g\Delta\rho/\rho_0$ is the “reduced gravity” ($g = \text{gravity} = 9.8 \text{ m s}^{-2}$, ρ is the density of seawater, with mean $\rho_0 = 1025 \text{ kg m}^{-3}$, and $\Delta\rho$ is the density difference between the active upper and motionless lower layers, typically a few kg m^{-3} . The long gravity wave speed is $c^2 = g'H$).
- $\tau = (\tau^x, \tau^y)$ is the surface wind stress, assumed to be felt entirely within the upper layer.

Adding more layers, the reduced gravity model can be generalized to represent a continuously-stratified ocean.

Differences from Yolande's waves:

- Off-equatorial (f not βy)
- The ocean has boundaries!

Sverdrup balance

Consider the steady, linear, vertically-integrated equations of motion in a single-active-layer (reduced gravity) context:

$$-fV = -g'Hh_x + \tau^x / \rho_0 \quad (1)$$

$$fU = -g'Hh_y + \tau^y / \rho_0 \quad (2)$$

$$U_x + V_y = 0 \quad (3)$$

The dynamics are Ekman + geostrophic:

$$\text{Geostrophic: } U_g = -g'Hh_y / f, \quad V_g = g'Hh_x / f \quad (4)$$

$$\text{Ekman: } U_E = \tau^y / f\rho_0, \quad V_E = -\tau^x / f\rho_0 \quad (5)$$

(Note that (1) and (2) can therefore be rewritten: $U = U_g + U_E$ and $V = V_g + V_E$).

$$\text{Curl (1) and (2), use (3) to get the Sverdrup balance: } \boxed{\beta V = \text{Curl}(\tau)} \quad (6)$$

$$\text{Use (3) to find } U: U_x = -V_y = \frac{-1}{\beta} \frac{\partial}{\partial y} \text{Curl}(\tau) \Rightarrow U = \frac{1}{\beta} \int_{x_E}^x \frac{\partial}{\partial y} \text{Curl}(\tau) dx \quad (7)$$

where x_E is the eastern boundary. Since the integration is westward, dx is negative.

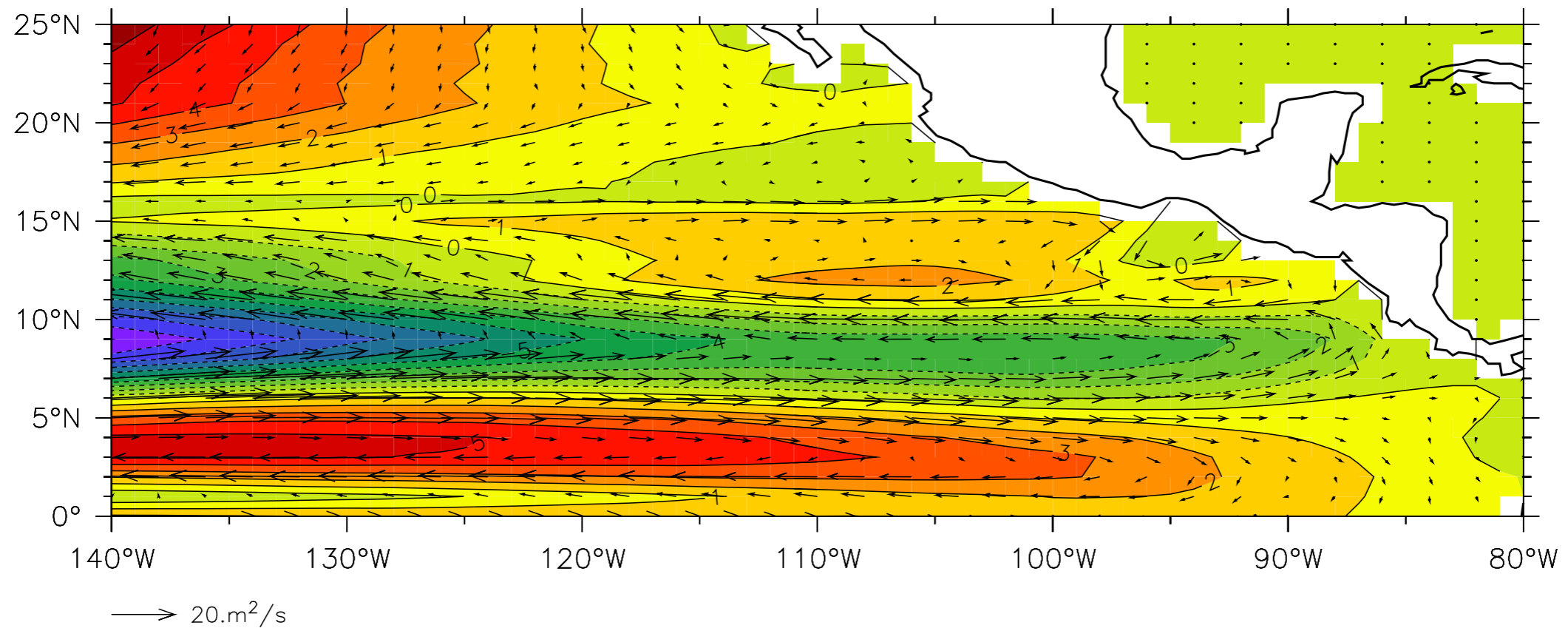
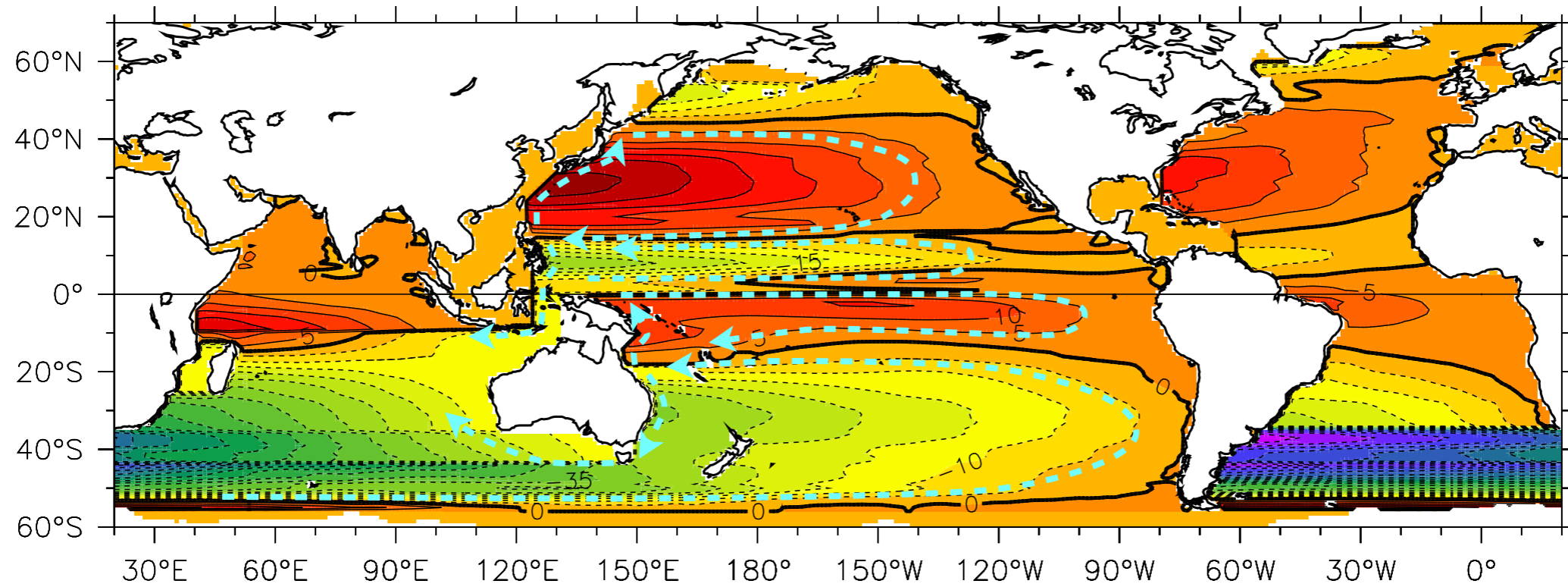
Since the vertically-integrated fluid is non-divergent (*i.e.*(3)), a streamfunction exists:

$$V = \psi_x, \quad U = -\psi_y, \quad \text{and} \quad \psi = \frac{-1}{\beta} \int_{x_E}^x \text{Curl}(\tau) dx \quad (8)$$

The integrals (7) and (8) require an eastern boundary condition, typically of no flow through the coast; for (8) this is satisfied by the choice $\psi = \text{constant}$ along the eastern boundary.

Note that none of (6), (7) or (8) contain the Coriolis parameter f , so the Sverdrup balance does not suffer the degeneracy of Ekman or geostrophic flow ((4) and (5)) at the equator.

Sverdrup streamfunction (Island Rule generalization)



Sverdrup balance (Island Rule) accurately predicts the transport of the Indonesian Throughflow from the wind alone!

Rossby waves

In “Fundamental” equations (1)-(3), take $u_t = v_t = 0$. The only explicit time variation is h_t in (3).

Physically, this assumes that the variability is “slow enough” that the velocity can be considered to be in steady balance with the winds and interface slope at each instant.

$$\begin{aligned}
 u_t - fv &= -g'h_x + \tau^x / \rho_0 H & (1) \\
 v_t + fu &= -g'h_y + \tau^y / \rho_0 H & (2) \\
 h_t + H(u_x + v_y) &= 0 & (3)
 \end{aligned}$$

Take the Curl of (1) and (2):

$$\underbrace{f(u_x + v_y)}_{-h_t/H} + \beta v = \text{Curl}(\tau) / H \quad (1)$$

Using $v = (g'h_x + \tau^x / H) / f$, $c^2 \equiv g'H$, and the vector identity $\frac{1}{f} \text{Curl}(\tau) + \frac{\beta}{f^2} \tau^x = \text{Curl}(\tau / f)$ (1) can be rewritten:

$$\text{Long Rossby eqn: } h_t - \left(\frac{\beta c^2}{f^2} \right) h_x = -\text{Curl}(\tau / f) \quad (2)$$

The long Rossby speed is $c_r = -\beta c^2 / f^2$. Note that c_r is always negative (westward).

(2) is a first-order PDE that is solved by integrating west along the Rossby wave ray paths. Since the left side of (2) has no y derivatives, these are due westward and each latitude is independent. The solution is the accumulation of $\text{Curl}(\tau / f)$ from the eastern boundary, moving west at speed c_r . An eastern boundary condition is required.

Long Rossby waves are the simplest time-dependent modification of the Sverdrup balance. (1) can be rewritten:

$$\underbrace{\beta V(t) = \text{Curl}(\tau(t))}_{\text{evolving Sverdrup balance}} + fh_t \quad (3)$$

Thus the Sverdrup circulation is the result of adjustment by Rossby waves, and (2) expresses the essential dynamics of low-frequency interior ocean circulation.

Ekman pumping

The reason the wind Curl, rather than the wind itself, appears as the forcing term for the Rossby wave equation is that it is the divergence of Ekman transport that produces the thermocline slopes (h_x). This divergence is:

$$\nabla \cdot \overline{\mathbf{U}}_{\mathbf{E}} = \frac{\partial U_E}{\partial x} + \frac{\partial V_E}{\partial y} = \left(\frac{\tau^y}{f} \right)_x - \left(\frac{\tau^x}{f} \right)_y = \frac{1}{f} \text{Curl}(\tau) + \frac{\beta}{f^2} \tau^x = \text{Curl}(\tau/f) . \quad (1)$$

$\text{Curl}(\tau/f) \equiv w_e$ is known as the “Ekman pumping velocity”.

This externally-imposed stretching or shortening of a water column changes its rotation (“vorticity”) as the column becomes wider or thinner and angular momentum is conserved.

Rossby waves are fundamentally the adjustment between local ($\zeta = v_x - u_y$) and planetary (f) rates of rotation, forced by the wind through Ekman pumping. The intimate connection between stretching and meridional motion can be seen in two ways: because of the equivalence of local and planetary vorticity, and because the Rossby wave term ($c_r h_x$) equals β/f times the meridional geostrophic transport $V_g = g' H h_x / f$.

Sverdrup balance works!

Rewrite Sverdrup balance

The dynamics considered here are assumed to be steady and linear and described in the vertical integral by the Sverdrup balance,

$$\beta V = \text{curl}(\tau). \quad (1)$$

Upper case symbols indicate vertically integrated velocities, and τ has been divided by background density. Decomposing the meridional velocity into geostrophic and Ekman parts, where $V_E = -\tau^\times/f$, and using the identity $\text{curl}(\tau/f) \equiv \text{curl}(\tau)/f + \beta\tau^\times/f^2$, allows rewriting (1) as

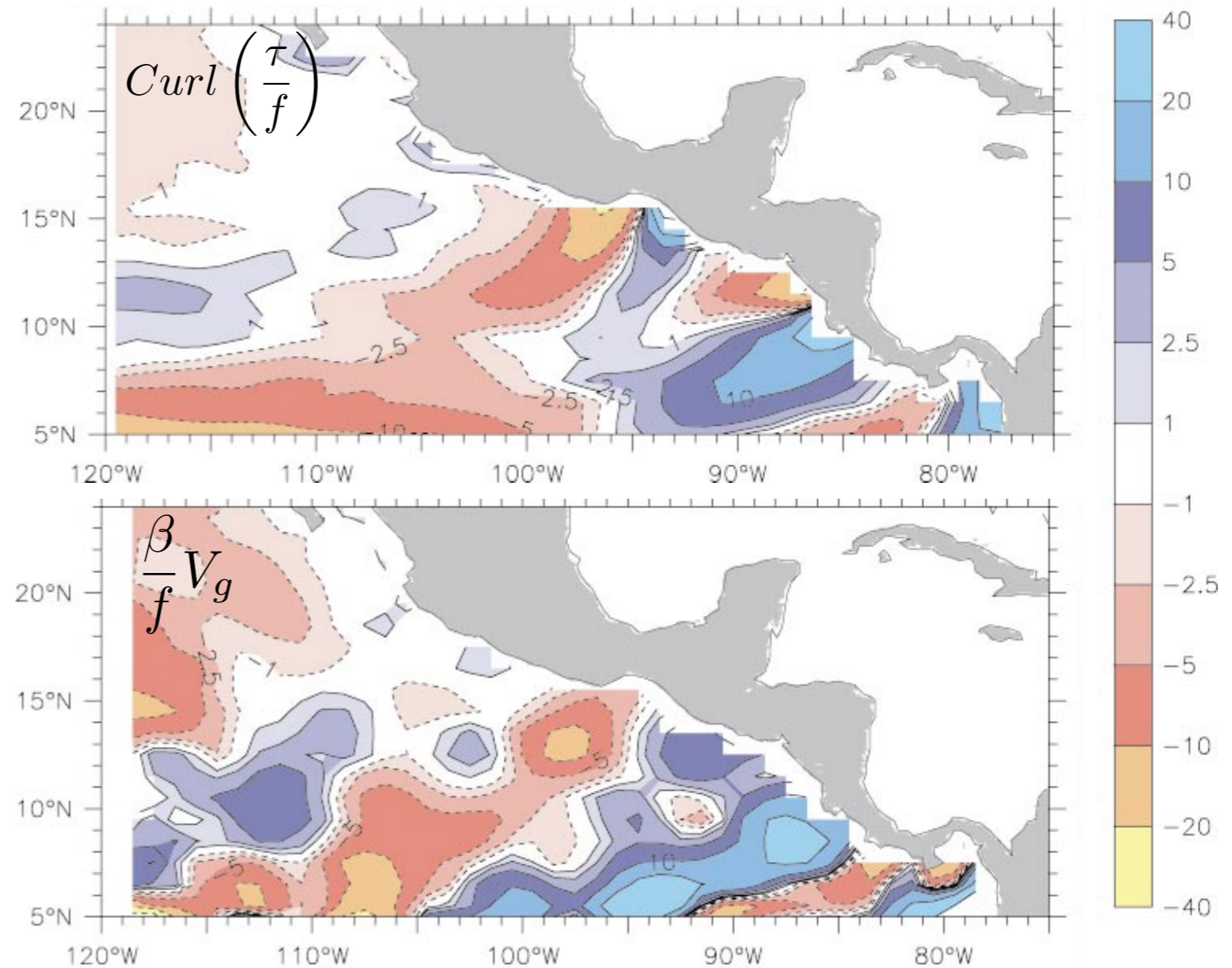
$$\frac{\beta}{f} V_g = \text{Curl} \left(\frac{\tau}{f} \right) \quad (2)$$

In (2) the geostrophic term on the left can be evaluated from the observed ocean data, and the term on the right from the observed winds, providing a convenient comparison between the independent XBT and scatterometer data sources.

Evaluate from ocean data

Evaluate from wind data

Blue = upwelling w_e (top), northward V_g (bottom): meters/month



Kessler (2002)

Well, almost. Where is the Costa Rica Dome?

Sverdrup balance works!

Rewrite Sverdrup balance

The dynamics considered here are assumed to be steady and linear and described in the vertical integral by the Sverdrup balance,

$$\beta V = \text{curl}(\tau). \quad (1)$$

Upper case symbols indicate vertically integrated velocities, and τ has been divided by background density. Decomposing the meridional velocity into geostrophic and Ekman parts, where $V_E = -\tau^\times/f$, and using the identity $\text{curl}(\tau/f) \equiv \text{curl}(\tau)/f + \beta\tau^\times/f^2$, allows rewriting (1) as

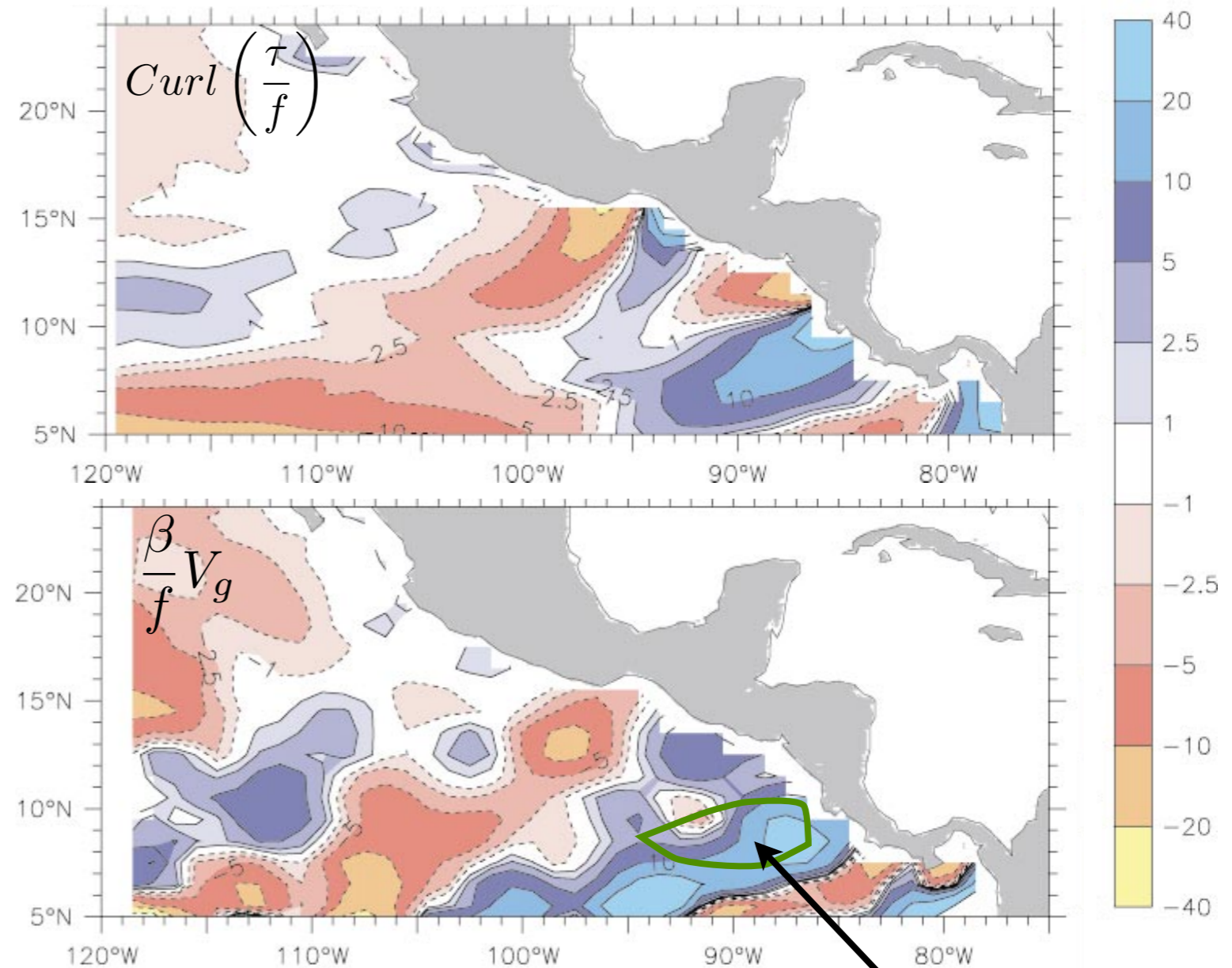
$$\frac{\beta}{f} V_g = \text{Curl} \left(\frac{\tau}{f} \right) \quad (2)$$

In (2) the geostrophic term on the left can be evaluated from the observed ocean data, and the term on the right from the observed winds, providing a convenient comparison between the independent XBT and scatterometer data sources.

Evaluate from
ocean data

Evaluate from
wind data

Blue = upwelling w_e (top), northward V_g (bottom): meters/month

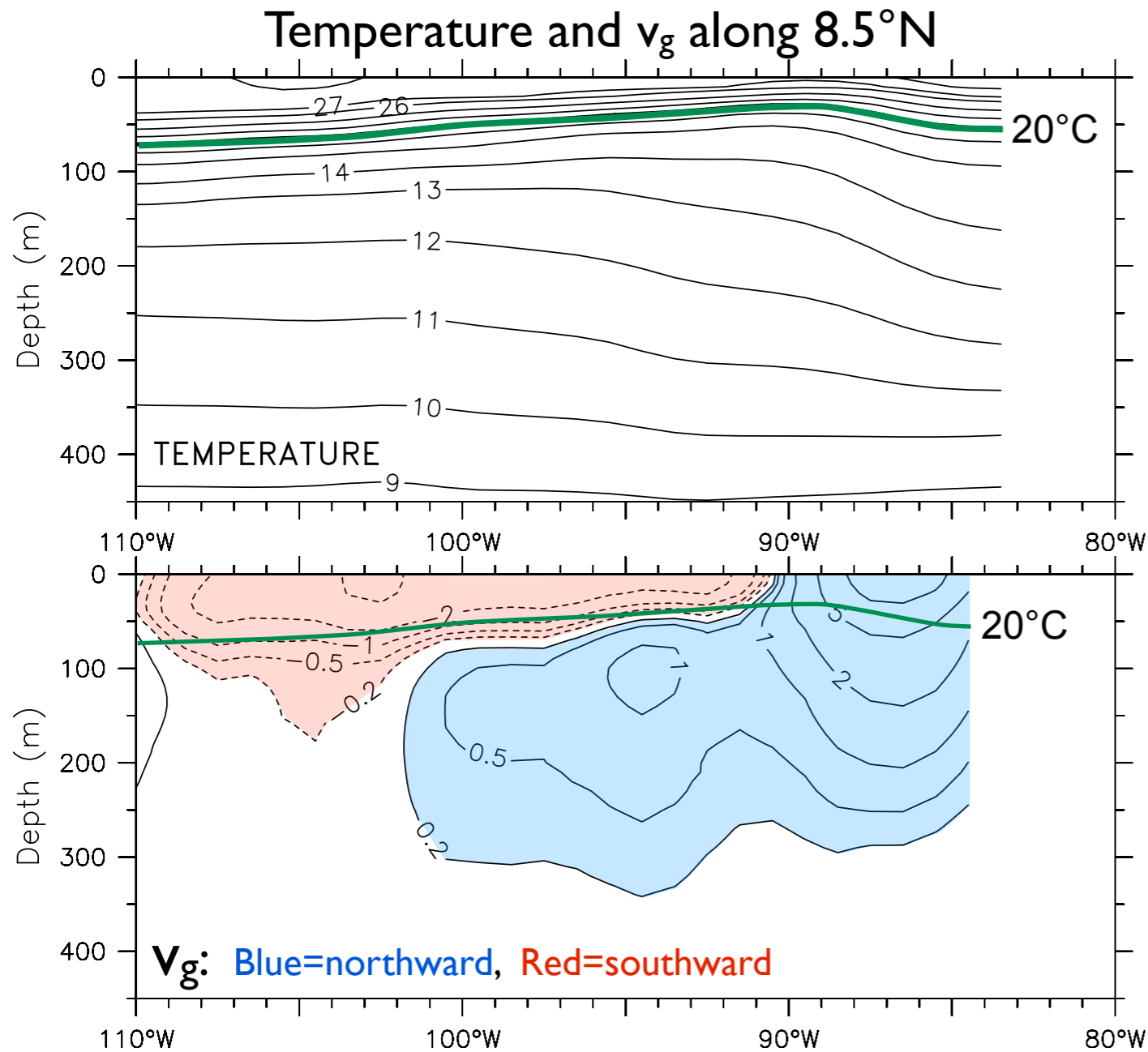


Kessler (2002)

These fields are zonal gradients: should change sign at the center of the CRD.

The Costa Rica Dome is a very shallow feature!

Subsurface flow below the dome is all northward. Why? And why does it matter?



Dynamic ht and geostrophic currents
Top: 0 rel 100m. Bottom: 100 rel 450m

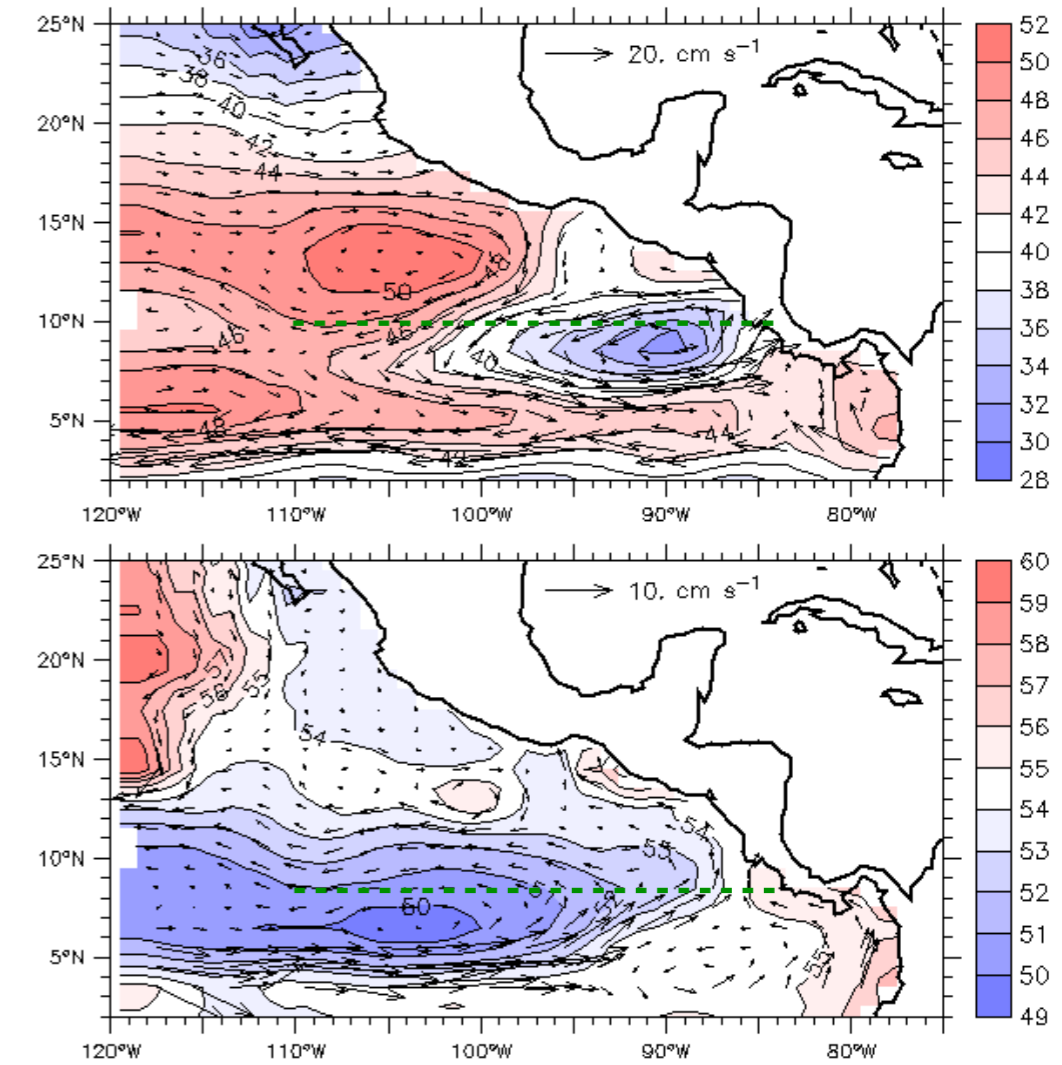
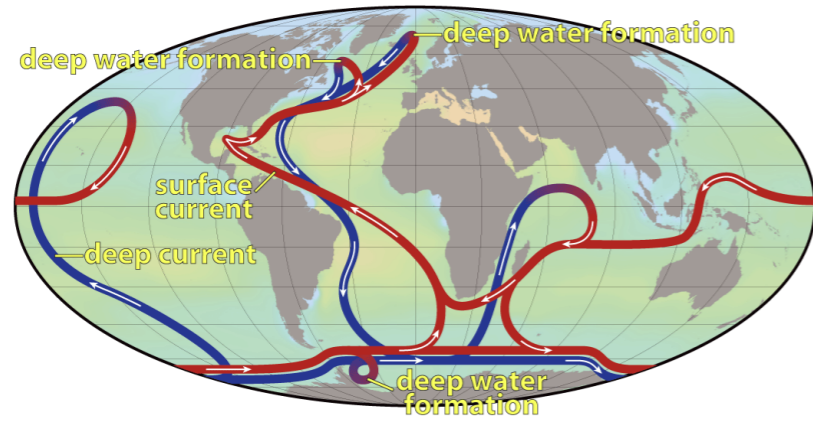
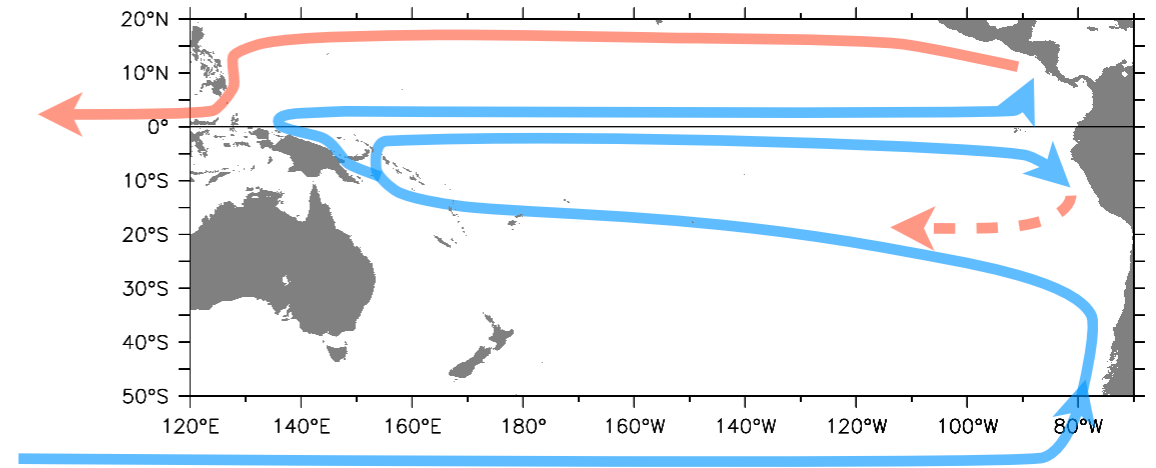


Fig. 8. Zonal sections of temperature (top) and meridional geostrophic current (bottom) along 8.5°N, from the coast (right edge) to 110°W. The contour interval for temperature is 1 °C from 8 to 14 °C, then 2 °C from 16 to 26 °C, then 1 °C from 27 to 29 °C; the 20 °C contour is darkened. In the bottom panel, northward current is indicated by solid contours, southward by dashed contours; the contour interval is every 5 cm within $\pm 15 \text{ cm s}^{-1}$, with additional contours at ± 1 and 2, ± 0.5 and $\pm 0.2 \text{ cm s}^{-1}$.

“Tsuchiya Jets” and the global conveyor belt

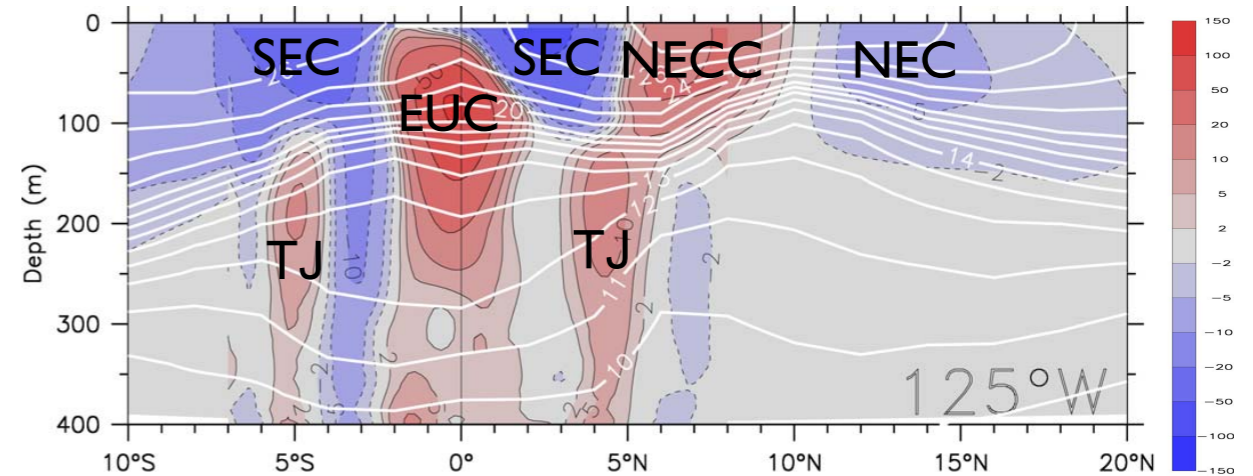


Cold water enters in the southeast
Warm water leaves in the Indonesian Throughflow



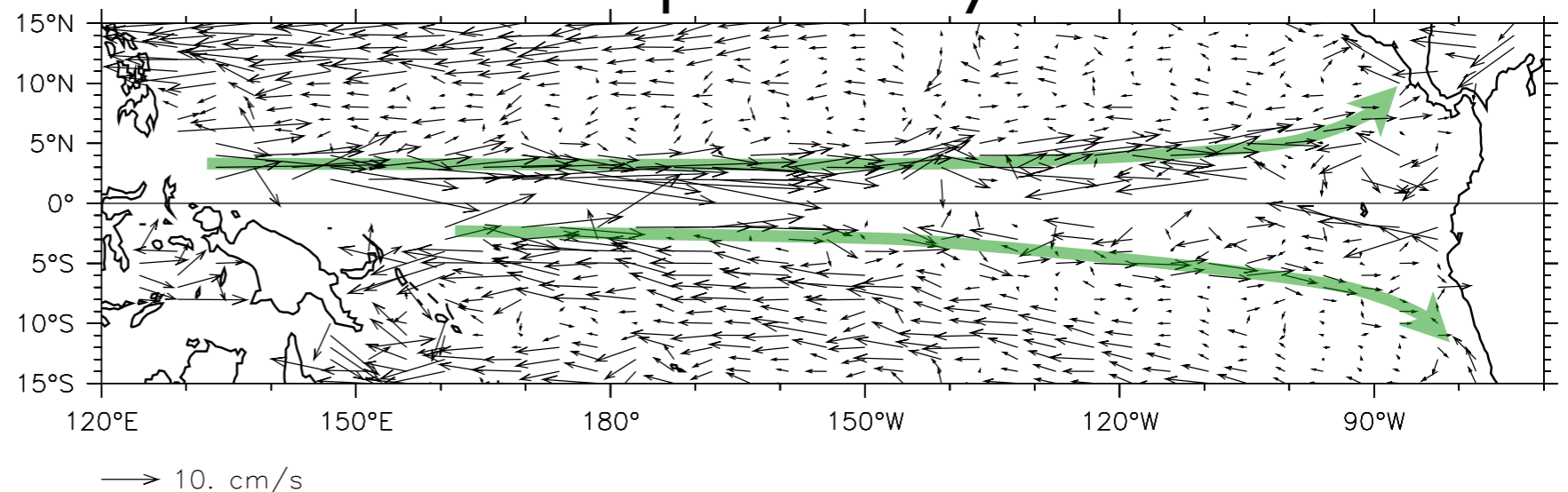
Water entering the South Pacific must
(a) be lifted through the thermocline, and
(b) cross the equator
Equatorial upwelling is shallow (next slide),
but CR Dome and Peru upwelling
reaches much deeper (beta-plume).

u (colors) and T (contours) at 125°W



The “Tsuchiya Jets” flow
across the entire Pacific
at about 13°C (2-300m),
feeding upwelling in the
CRD and Peru.

Geostrophic velocity at 200m



The Costa Rica Dome and Peru upwelling reach deep into the water column (equatorial upwelling is shallow)

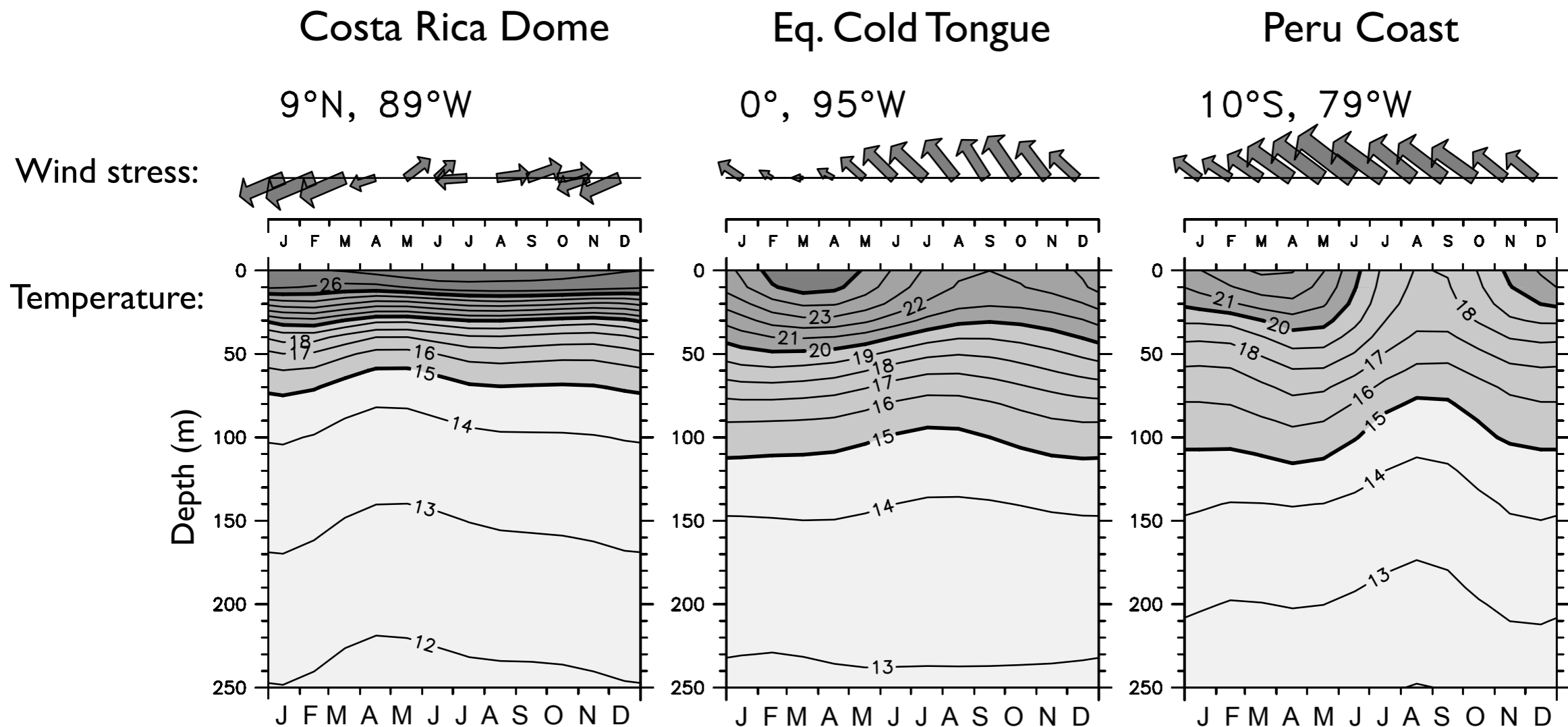


Fig. 9. Average annual cycle of wind stress vectors (top panels) and temperature (bottom panels) at the center of the Costa Rica Dome (9°N, 89°W; left), the equatorial cold tongue (0°W, 95°W; middle) and the Peru coastal upwelling (10°S, 79°W; right). Winds are the ERS scatterometer winds over 1991–2000, and both the length and thickness of the vectors increases with magnitude; the largest vector (June at the coast of Peru) has a magnitude of 5.8 N m^{-2} . Temperatures are from the AOML XBT data set.

Explaining this variety of behavior is good dynamical problem for a smart student!

Time-dependence ... Eddies, and the annual cycle

(come back to the eastern Pacific)

Tehuantepec and Papagayo eddies are dominantly anti-cyclonic

Eddy trajectories:
 Red=cyclonic
 Blue=anti-cyclonic

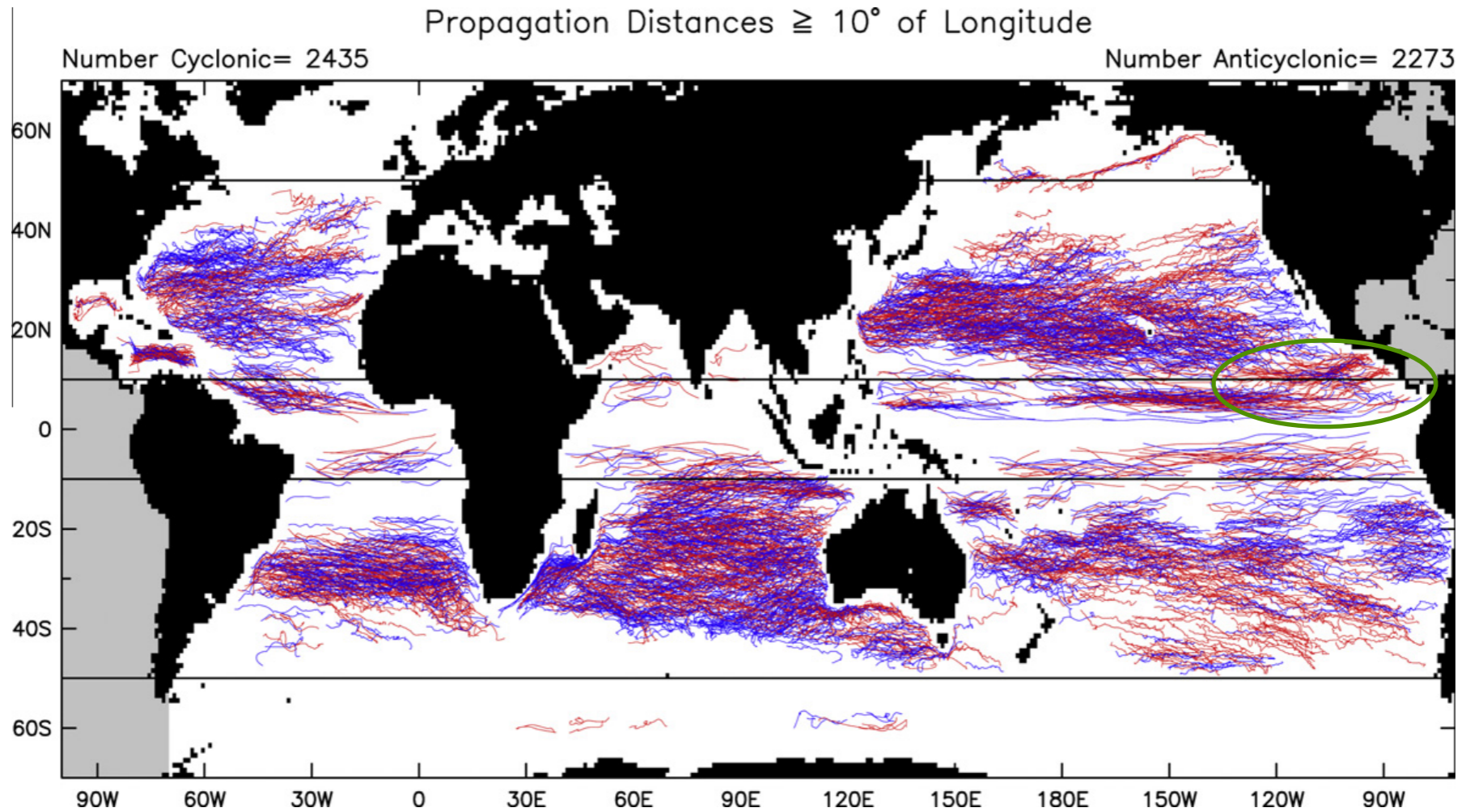
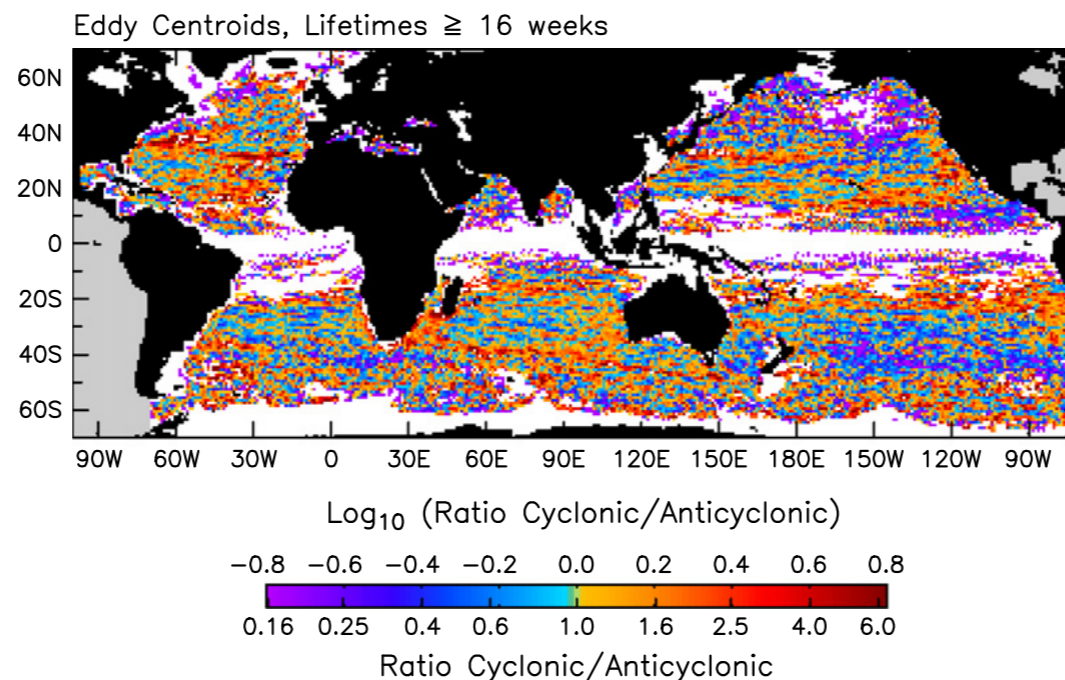


Fig. 18. The trajectories of all of the 2435 cyclonic (blue lines) and 2273 anticyclonic (red lines) eddies over the 16-year period October 1992–December 2008 that had lifetimes ≥ 16 weeks and propagated westward a minimum of 10° of longitude. The horizontal lines show the latitude ranges of 10° – 50° that were considered for the analyses in Figs 19 and 20

Ratio **cyclonic**/**anti-cyclonic**:



Chelton et al (2011)

Fig. 8. The ratio of the numbers of cyclonic to anticyclonic eddy centroids for eddies with lifetimes ≥ 16 weeks that propagated through each $1^\circ \times 1^\circ$ region over the 16-year period October 1992–December 2008. A logarithmic scale is used for the color bar in order to give equal emphasis to the ratios r and $1/r$.

Why are EP warm pool eddies dominantly anti-cyclonic?

1. Mechanisms at the forcing timescale.

Two hypotheses in the literature

Inertial turning of wind jet

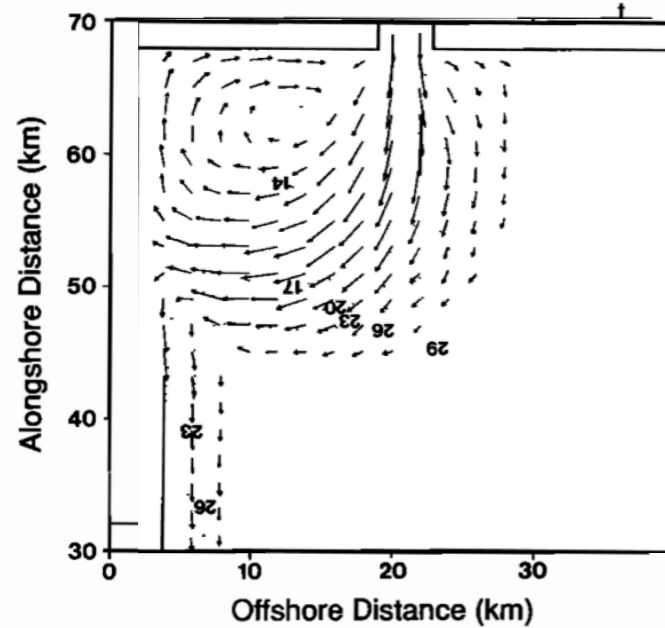


Fig. 6. Plan views of numerically calculated surface velocity and density for a surface flow exiting from a channel. The density is plotted in units of $0.1 \sigma_t$; only the difference is meaningful. The velocity scale is equal to 50 cm s^{-1} in one grid length [after Wang, 1987].

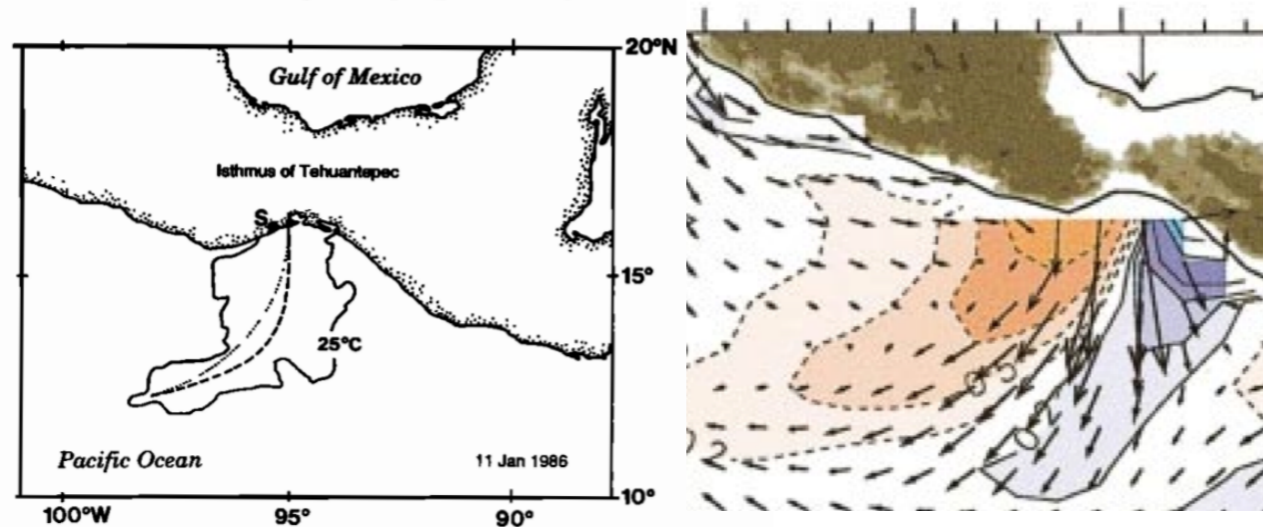
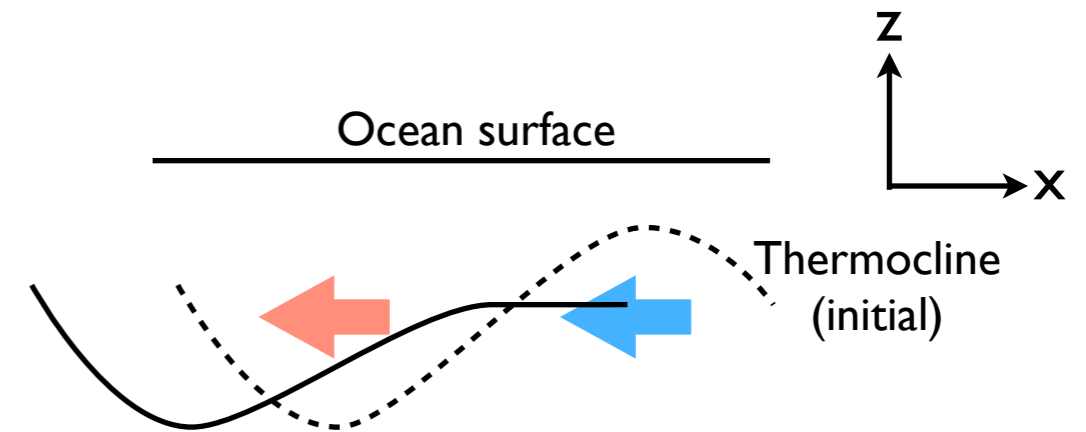
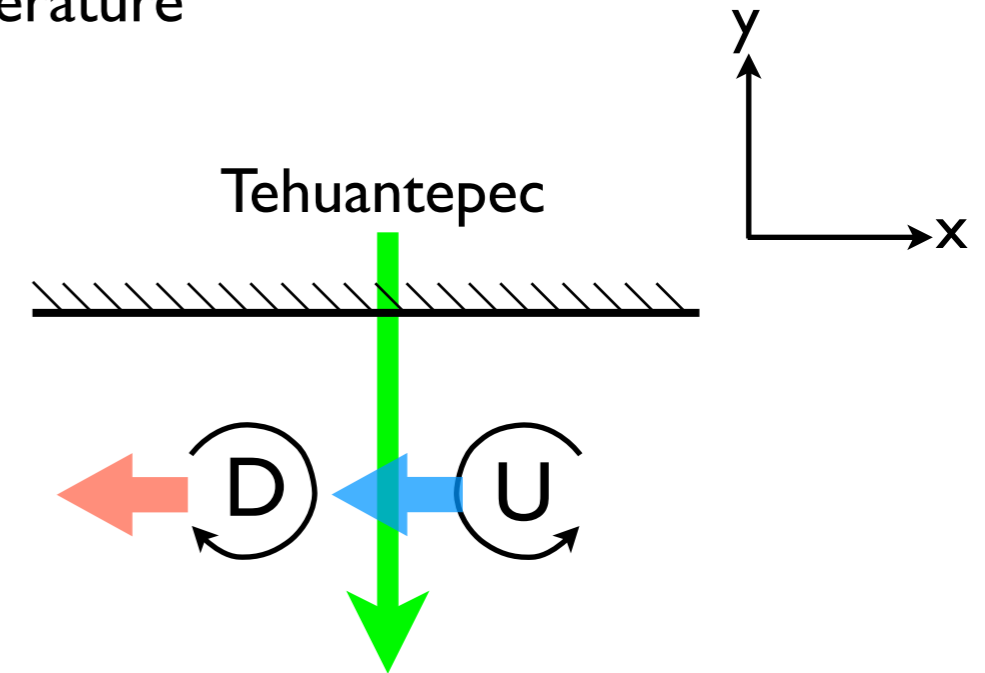


Fig. 7. Map showing the approximate location of the 25°C isotherm in the Gulf of Tehuantepec on January 11, 1986. The dashed line is an estimated axis for the wind jet path. The dotted line is the arc of a circle with radius of $419 \text{ km} \approx U/f = \text{inertial radius}$. The tangent to the arc is north-south at the coast. The symbol S stands for Salina Cruz.

(Clarke 1988)

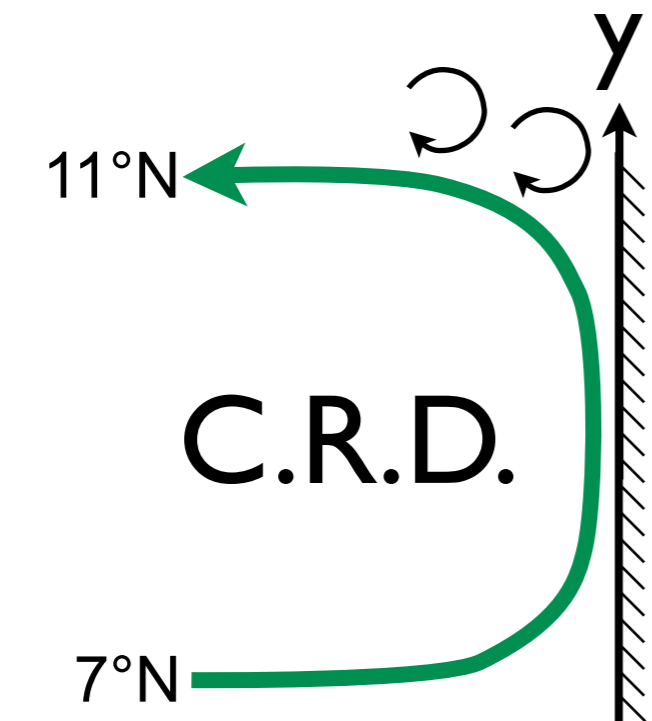


Tehuantepec jet produces both C and A-C eddies. Stirring under strong jet winds deepens shallow upwelled (cyclonic) eddy as it propagates, leaves deep anti-cyclonic eddy unchanged. (McCreary et al 1989, Trasviña et al 1995)

Why are EP warm pool eddies dominantly anti-cyclonic?

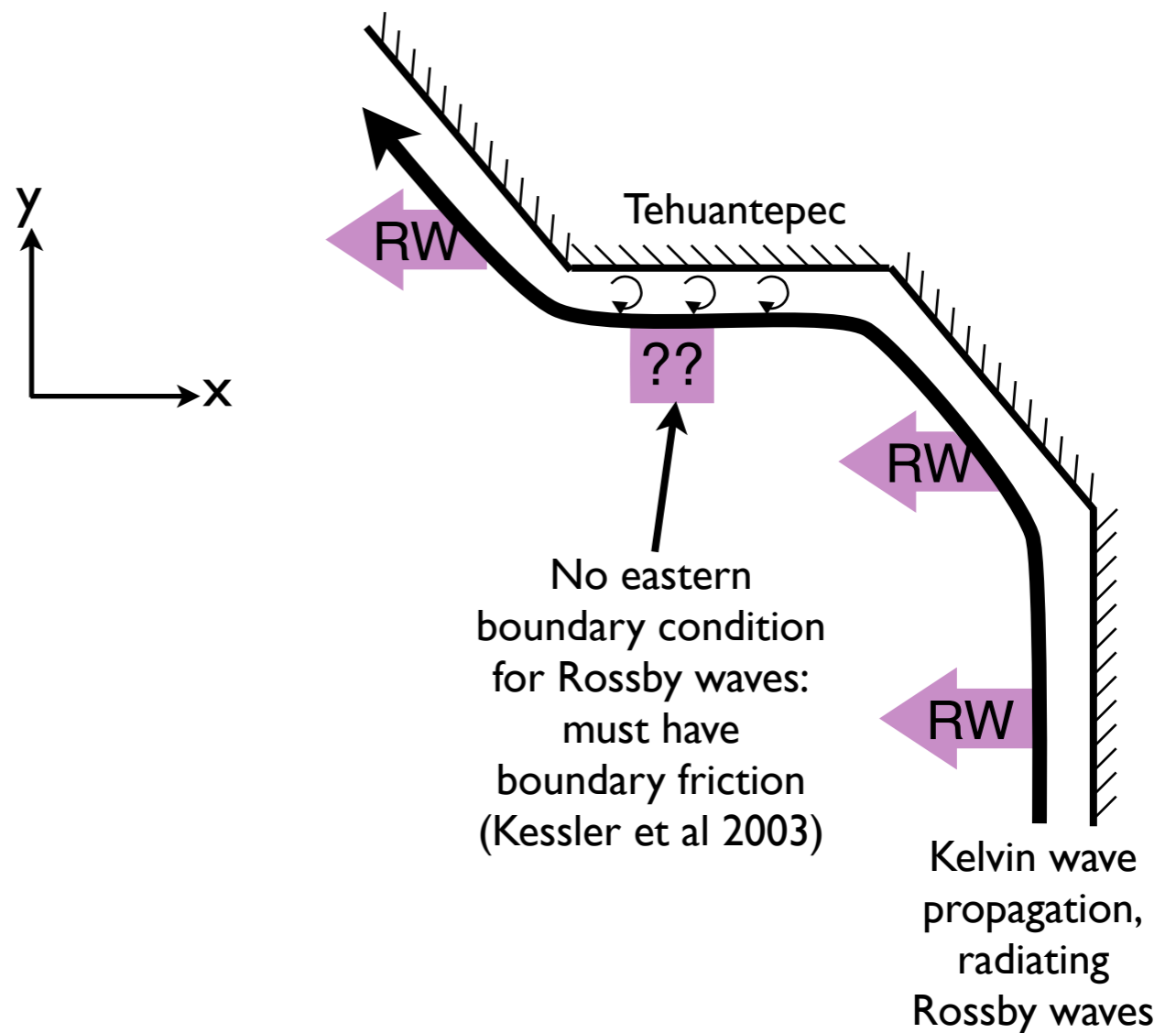
2. Can A-C eddies be generated without eddy-timescale wind forcing?

Two hypotheses in the literature



$$\zeta + f = \text{constant}$$

Water column arrives with initial vorticity of f at 7°N . Advected north around CRD, it must acquire anticyclonic relative vorticity: shed A-C eddies. (Hansen and Maul 1991) (also see Zamudio et al 2001)



These mechanisms allow eddy generation in the summer!

Other non-linear effects on eddies

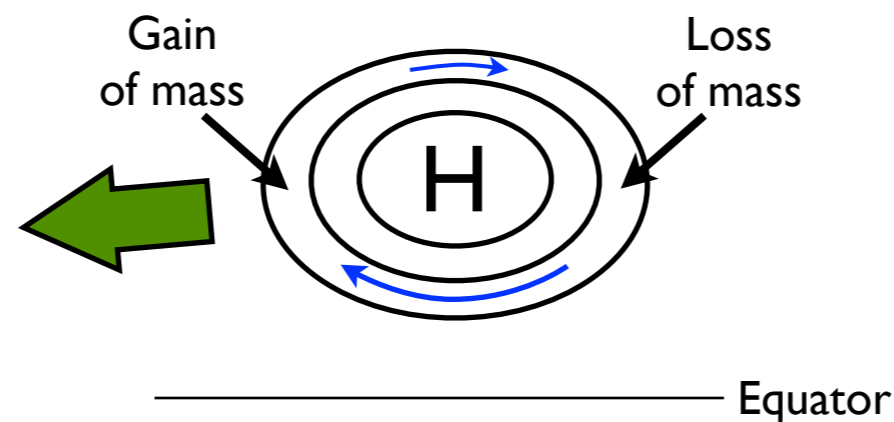
- If the anomaly h is a substantial fraction of the mean depth H , then A-C eddies will propagate faster:

$$c^2 = g'H \Rightarrow c^2 = g'(H + h)$$

- If the rotation speed is large, then the relative vorticity ζ may be important:

$$\text{Curl} \left(\frac{\tau}{f} \right) \Rightarrow \text{Curl} \left(\frac{\tau}{f + \zeta} \right)$$

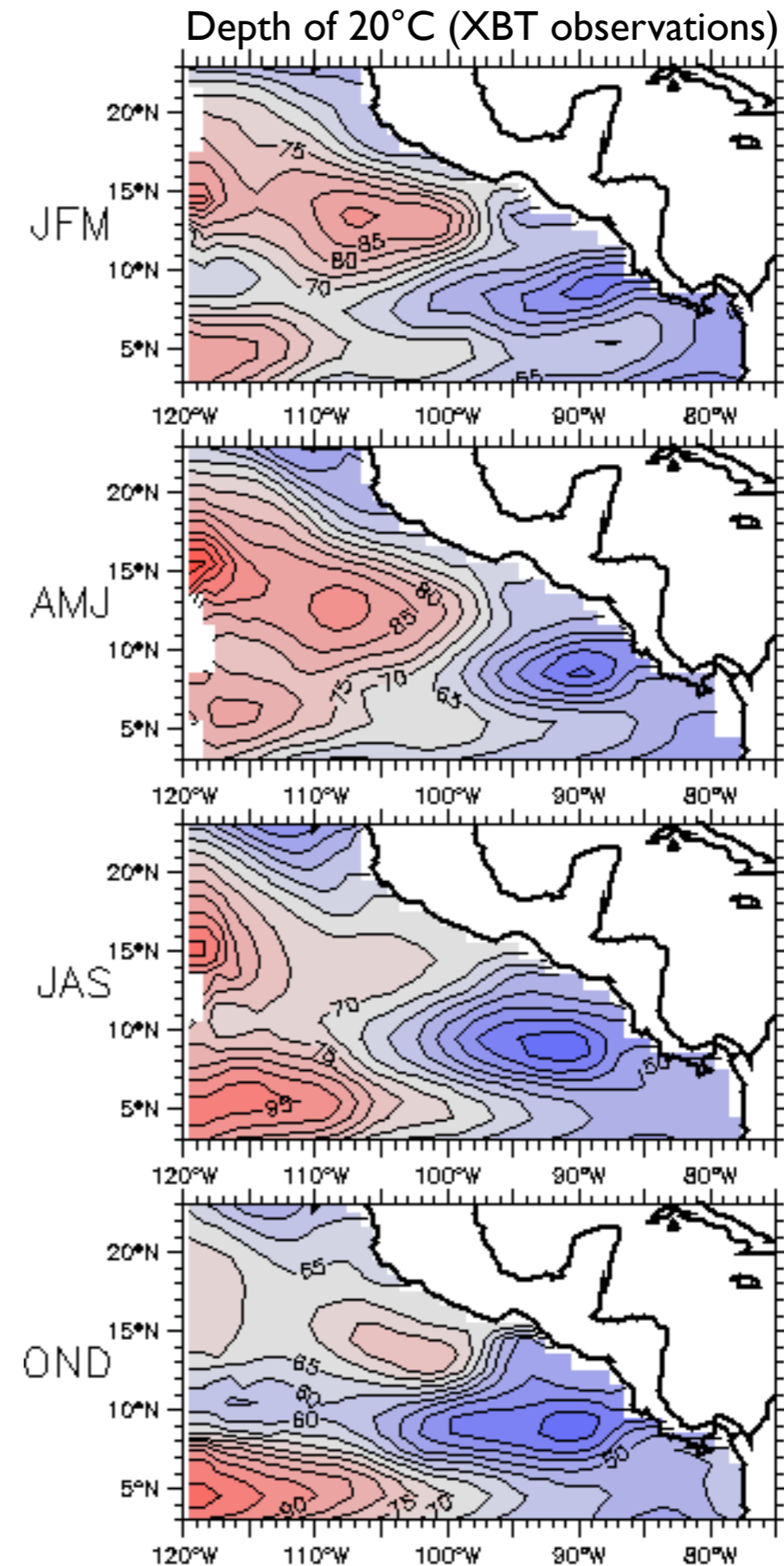
- Eddy self-advection can transport properties (Rossby model is wave-like). Such A-C eddies also drift slightly equatorward (observed).



- Large anti-cyclones can spin off cyclonic eddies.

Is the mean “Tehuantepec Bowl” simply aliased A-C eddies?

- Costa Rica Dome exists all year (different sources of Curl)
- Tehuantepec Bowl weakens in summer (but maybe this doesn't matter for SST)



Annual cycle of gap winds

The gap winds max is in winter, but the Tehuantepec and Papagayo jets have a secondary peak in mid-summer.

(Probably related to Azores-Bermuda high.)

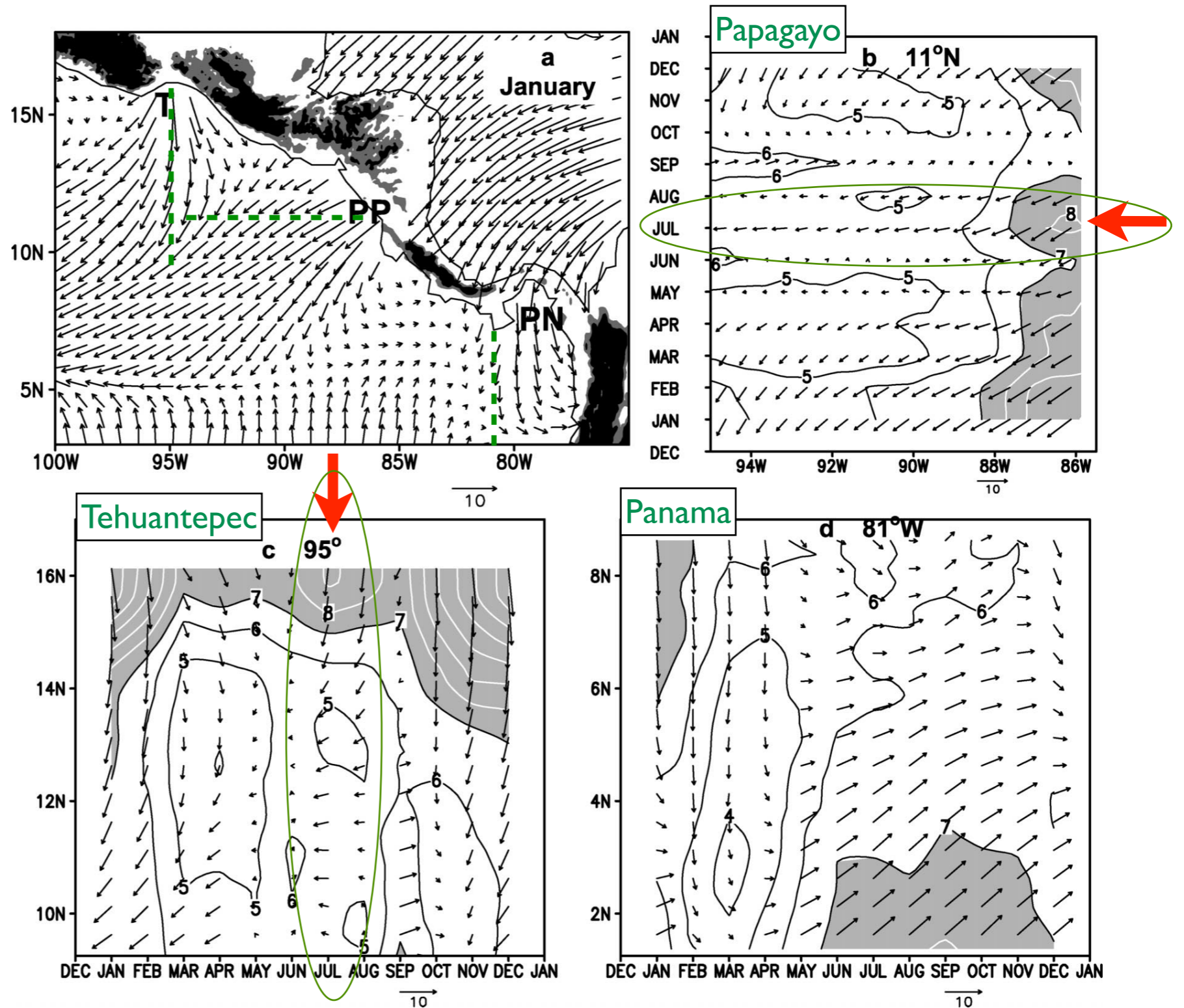
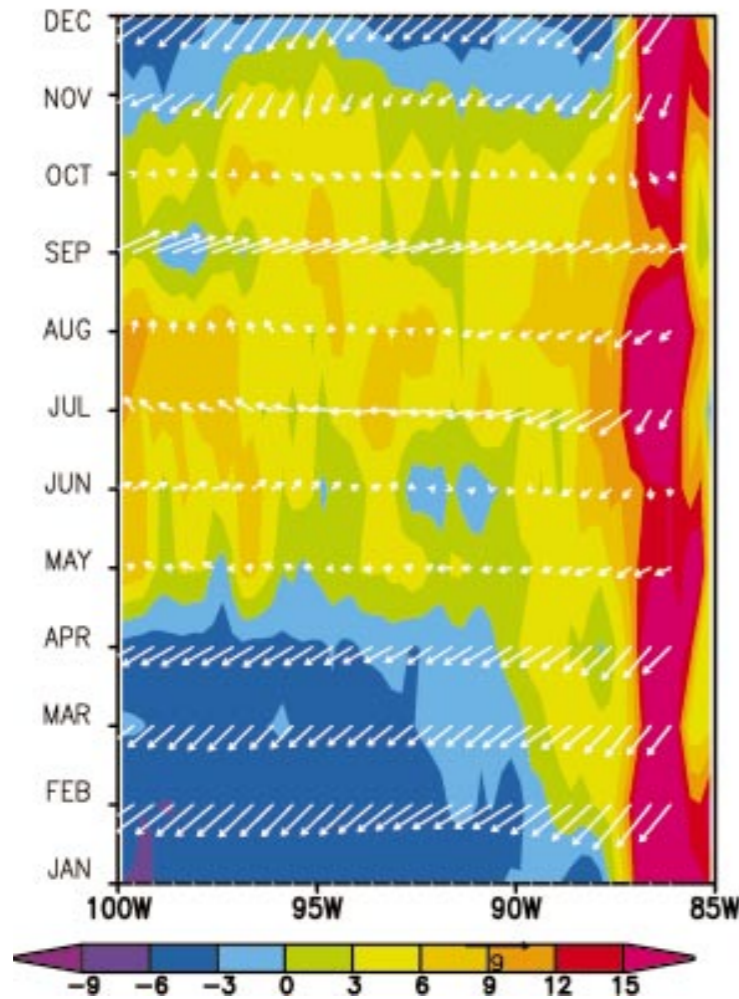


FIG. 1. (a) Wind jets over the Gulfs of Tehuantepec (T), Papagayo (PP), and Panama (PN) in the QuikSCAT surface wind velocity (m s^{-1}) climatology for Jan. (b) Longitude–time section of wind velocity (u, v) and scalar speed (contours; shade $> 7 \text{ m s}^{-1}$) at 11°N (Papagayo gap). Latitude–time sections of wind velocity and scalar speed (contours; shade $> 7 \text{ m s}^{-1}$) (c) at 95°W (Tehuantepec gap), and (d) at 81°W (Panama gap). In (a) the light and dark shades denote topography greater than 500 and 1000 m, respectively.

Annual cycle of winds

Ekman pumping at 10°N



Away from the coast, the annual cycle is a simple north-south motion of the ITCZ.

Positive curl at Papagayo is increased in summer by ITCZ westerlies to its south: not much annual variation.

➔ CRD remains shallow all year.

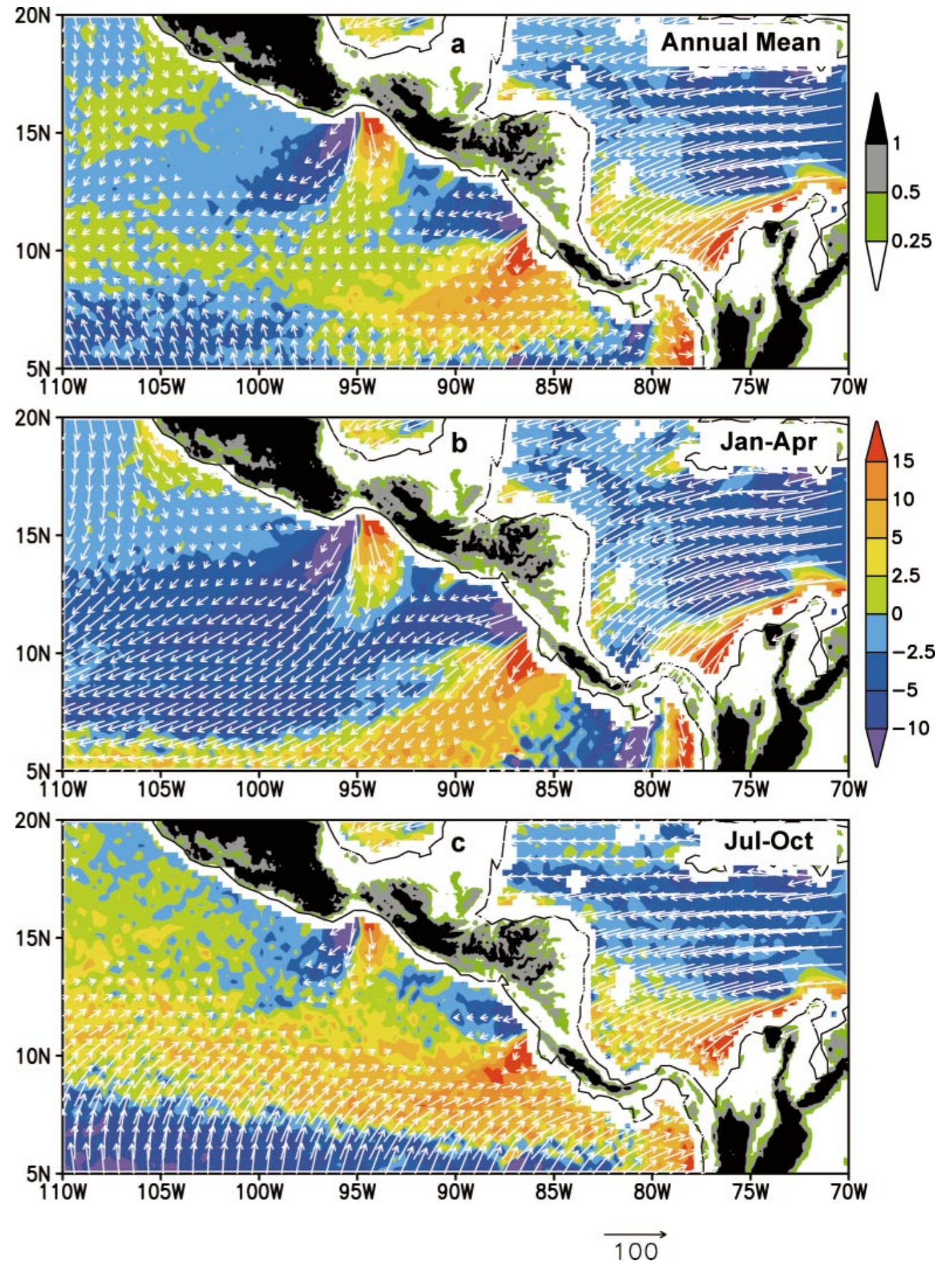
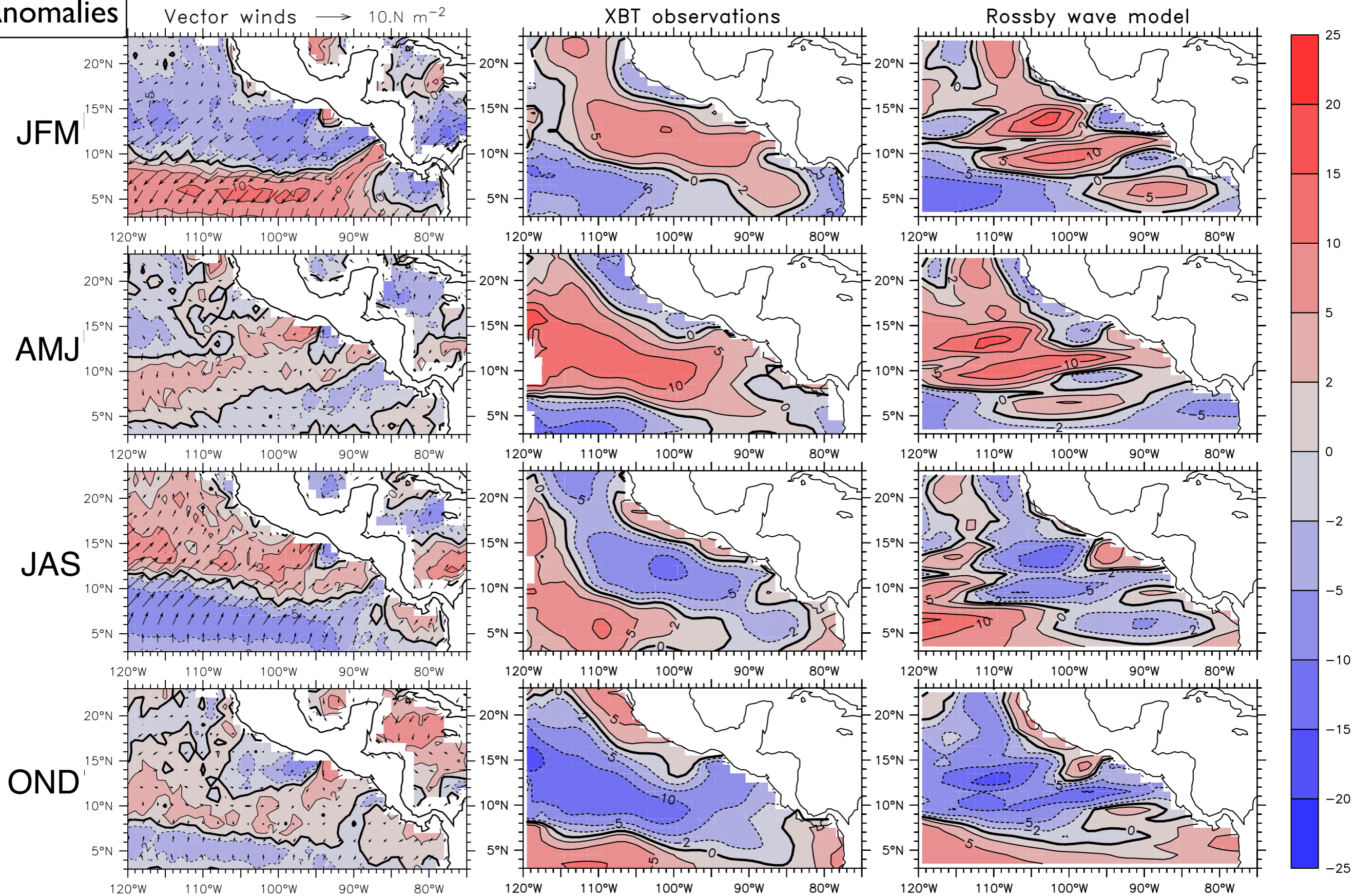


FIG. 3. QuikSCAT pseudo-wind stress (vectors in $\text{m}^2 \text{s}^{-2}$) and Ekman pumping velocity (shade in 10^{-6}m s^{-1}) climatology: (a) annual mean, (b) Jan-Apr, and (c) Jul-Oct. Land orography (km) is plotted in color shading.

A linear Rossby model represents observed annual Z20 fluctuations

$$h_t + c_r h_x + Rh = -\text{Curl} \left(\frac{\tau}{f} \right)$$

Anomalies



Observed seasonal cycle of upper-level currents

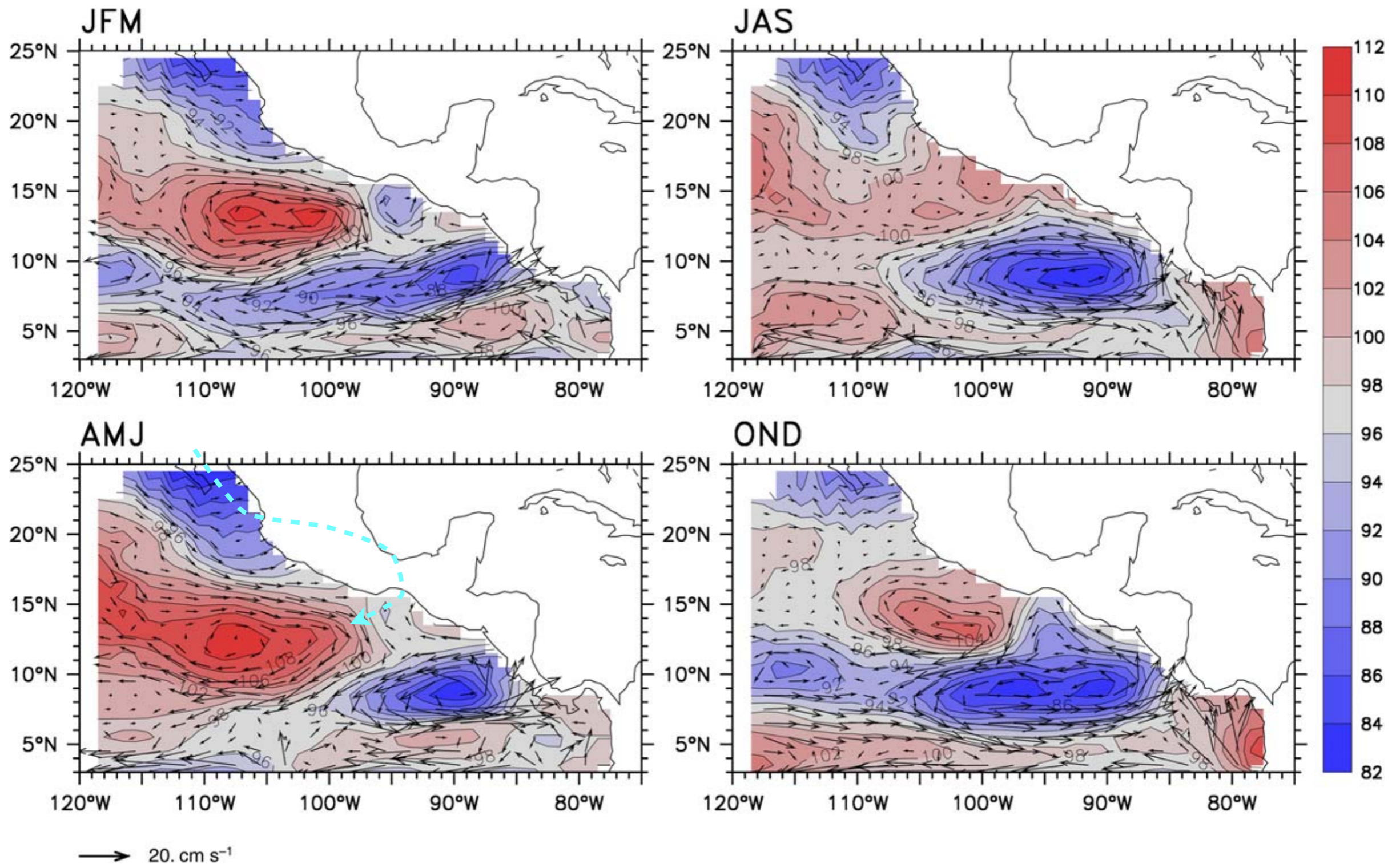
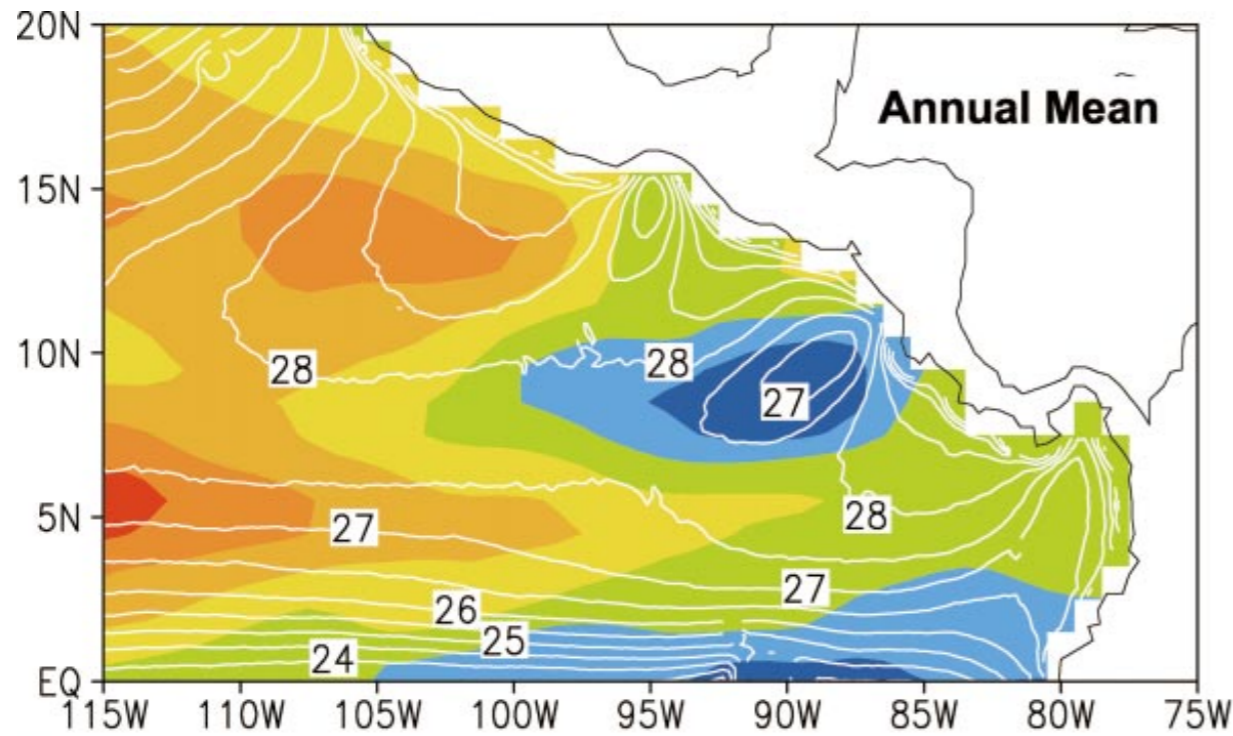


Fig. 7. Annual cycle of surface dynamic height and geostrophic current (relative to 450 m), shown as four average seasons. Red colors indicate high dynamic heights, blue low. The contour interval is 2 dyn cm. The scale vector for geostrophic currents is at lower left. The dynamic height contours shown here have very nearly the same patterns as contours of 20 °C depth for the corresponding season.

SST and thermocline depth are only related in winter

(Except for the Costa Rica Dome)

Colors = Thermocline depth
White contours = SST



Little apparent effect of Tehuantepec Bowl thermocline depth variations on SST

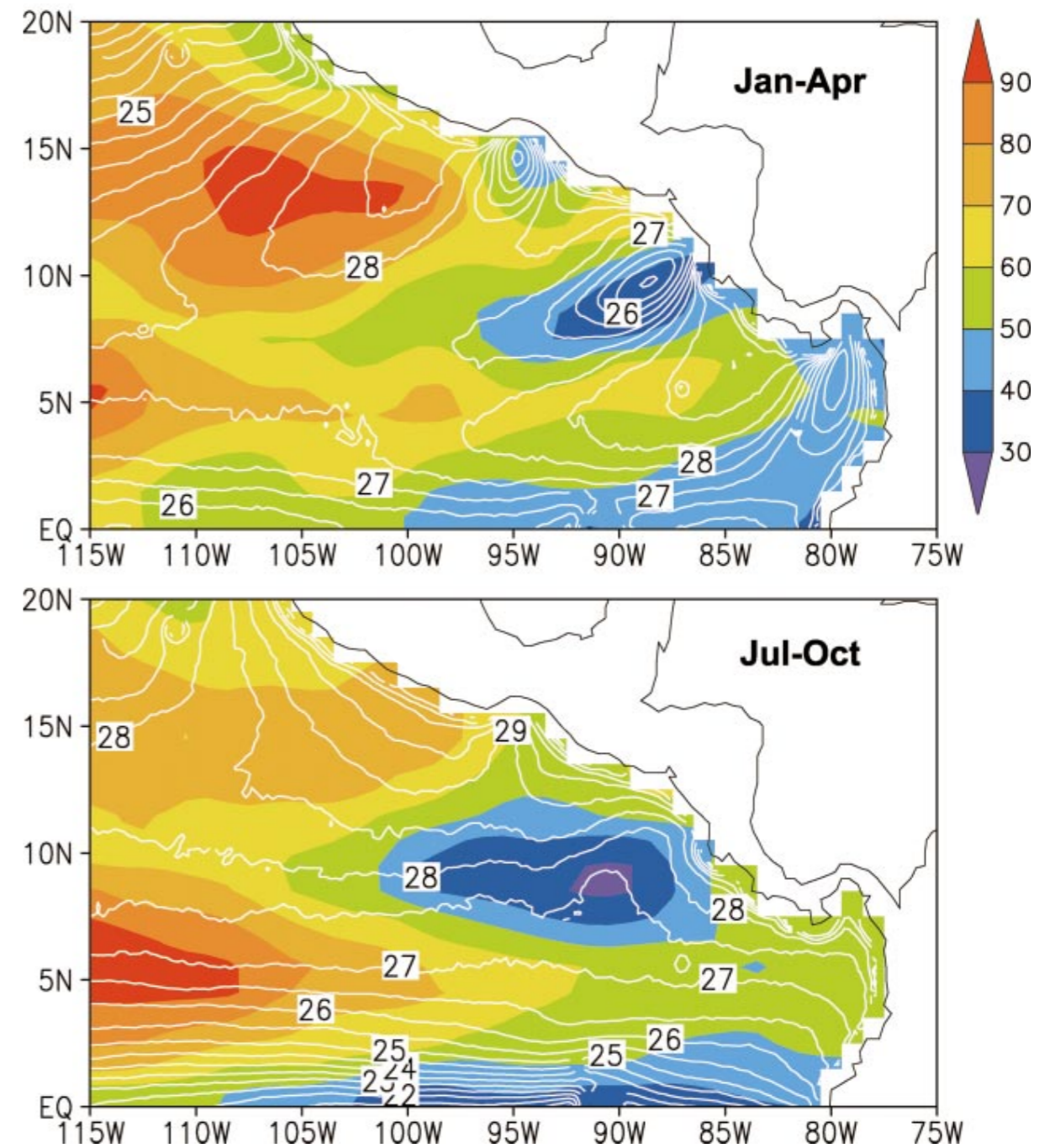


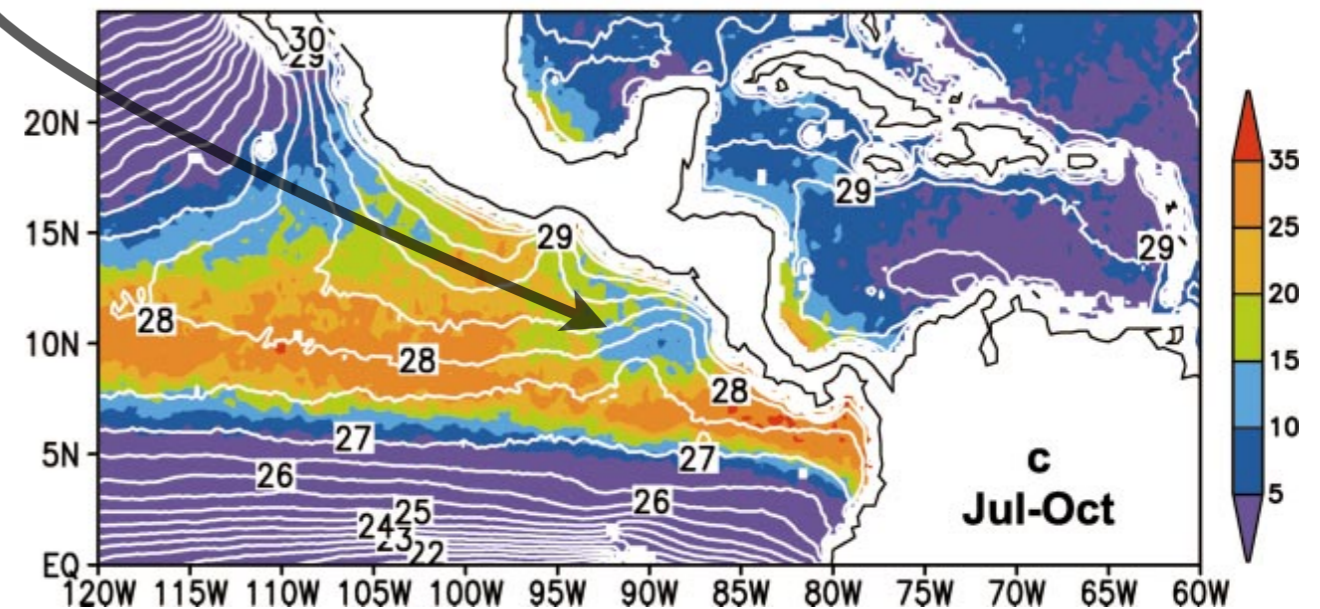
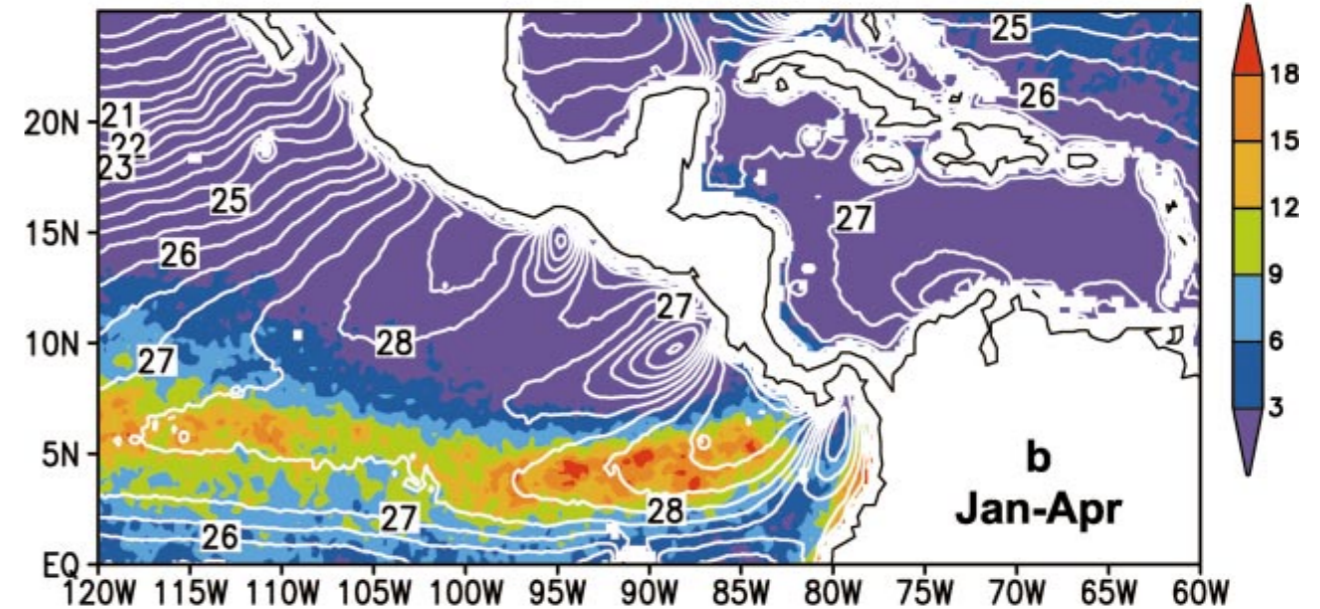
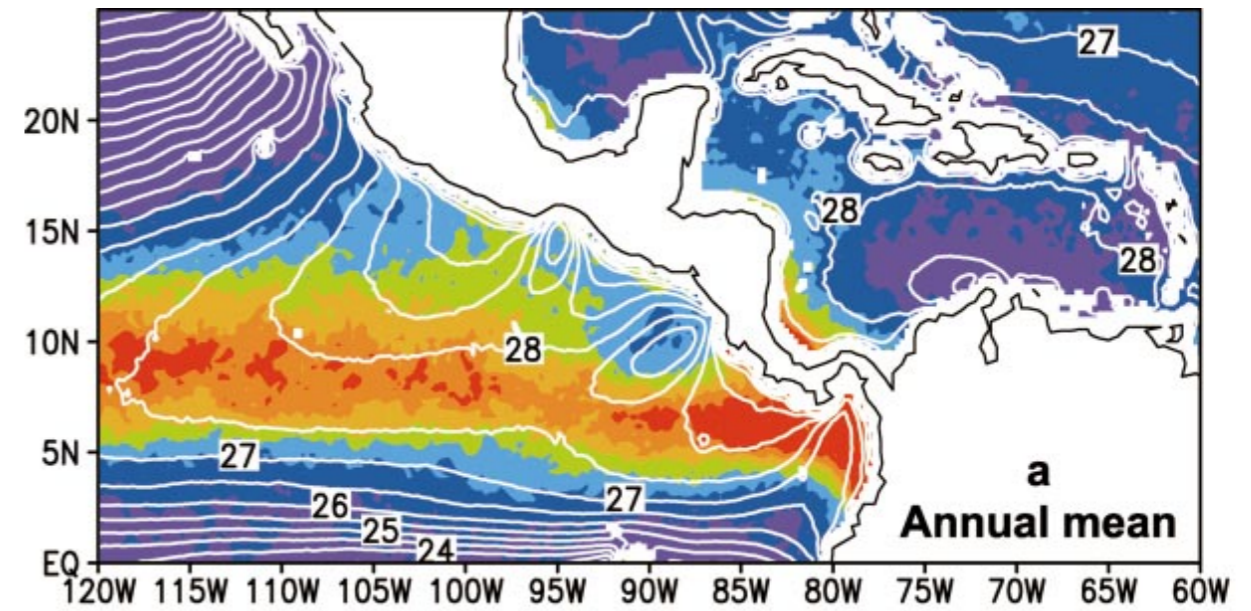
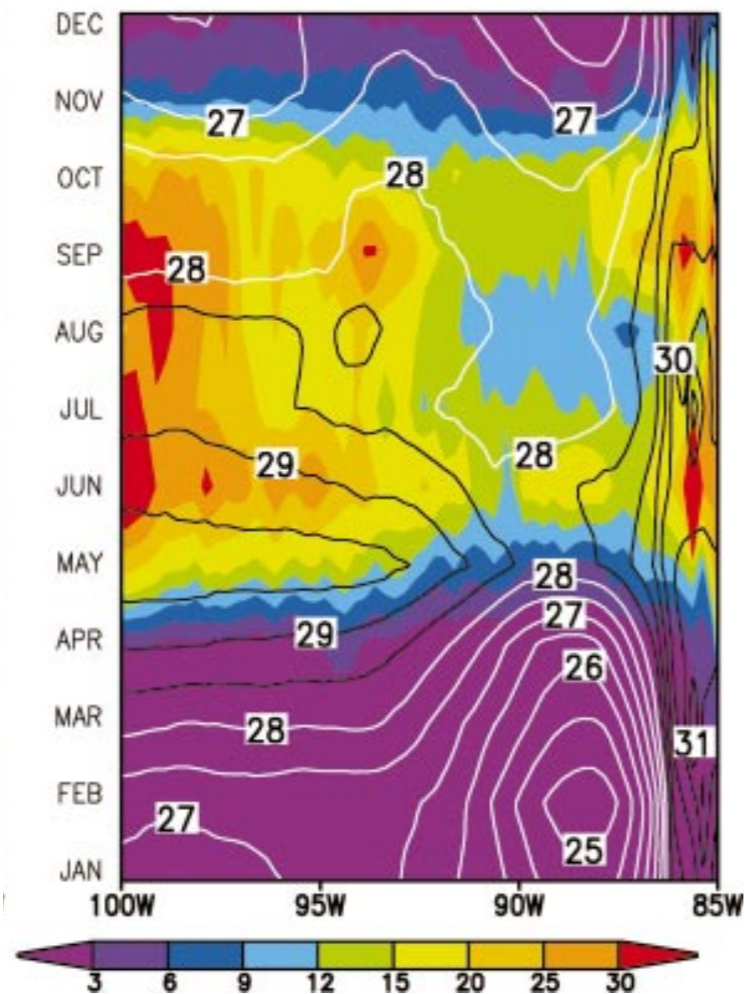
FIG. 4. Climatology of SST (contours at intervals of 0.5°C) and the 20°C isotherm depth (color in m): (a) Annual mean, (b) Jan–Apr, and (c) Jul–Oct.

Precipitation partly controlled by SST

Little effect of SST on precip in winter (no precip!), but the Costa Rica Dome makes a summer hole in precip pattern.

SST: white contours. Precipitation: colors (mm/day)

Precip (mm/day, colors), SST (contours)



Summer precip hole due to cool SST

Jul-Oct Precip: radar and infrared

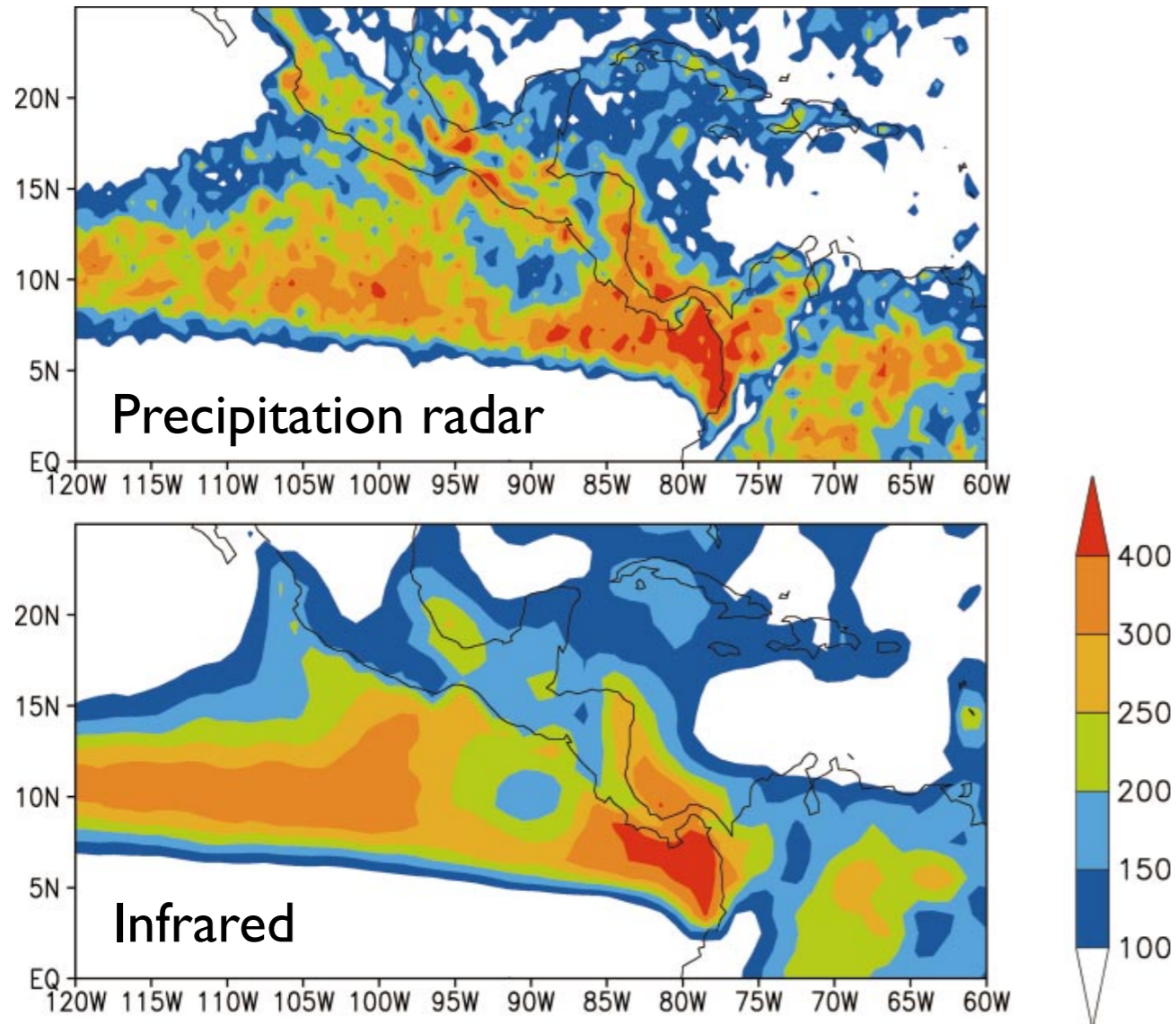


FIG. 10. Jul–Oct precipitation (mm month⁻¹) based on the (top) TRMM PR (3A25G2) and (bottom) infrared (3B43) measurements.

Aug 99 precip: regional model

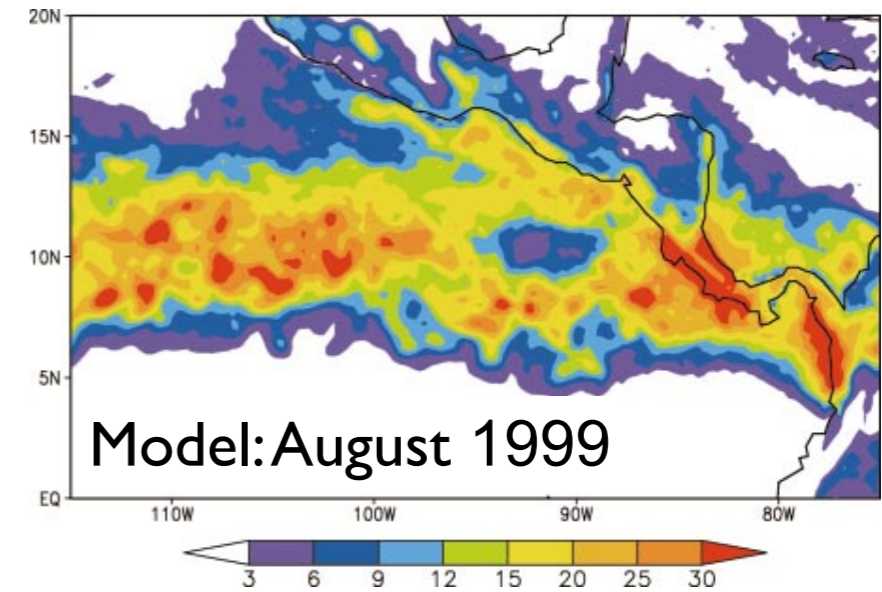


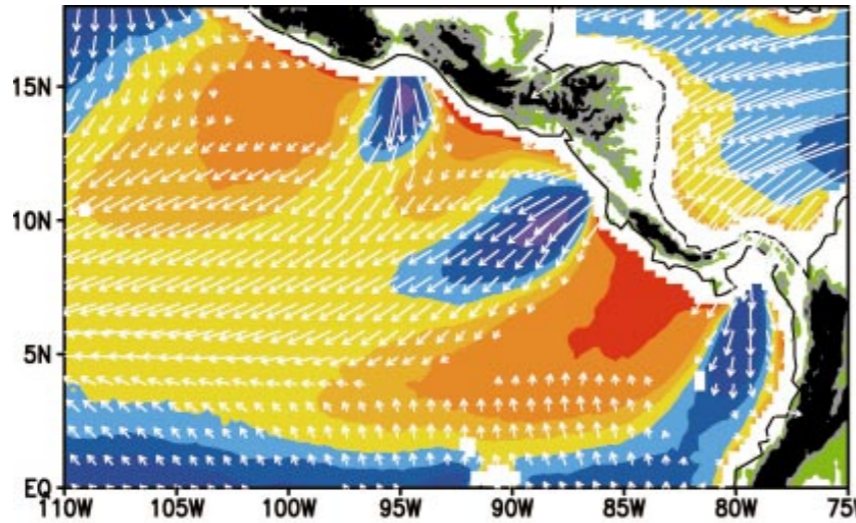
FIG. 11. Precipitation (mm day⁻¹) in a regional atmospheric model, averaged for Aug 1999.

Same result in model without orography

Productivity: stirring in winter, shallow thermocline in summer

Jan-Mar climatology

Winds
and
SST



Winds
and
chlorophyll

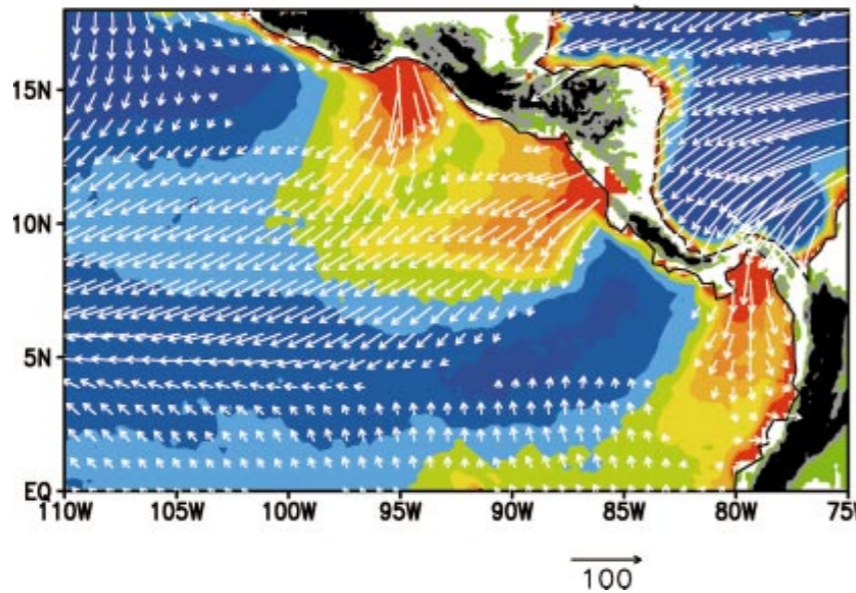


FIG. 6. Jan-Mar climatology: QuikSCAT pseudo-wind stressors; $m^2 s^{-2}$): (top) TMI SST ($^{\circ}C$) and (bottom) SeaWiFS chlor in natural logarithm ($mg m^{-3}$).

Chlorophyll (colors), SSH (contours)

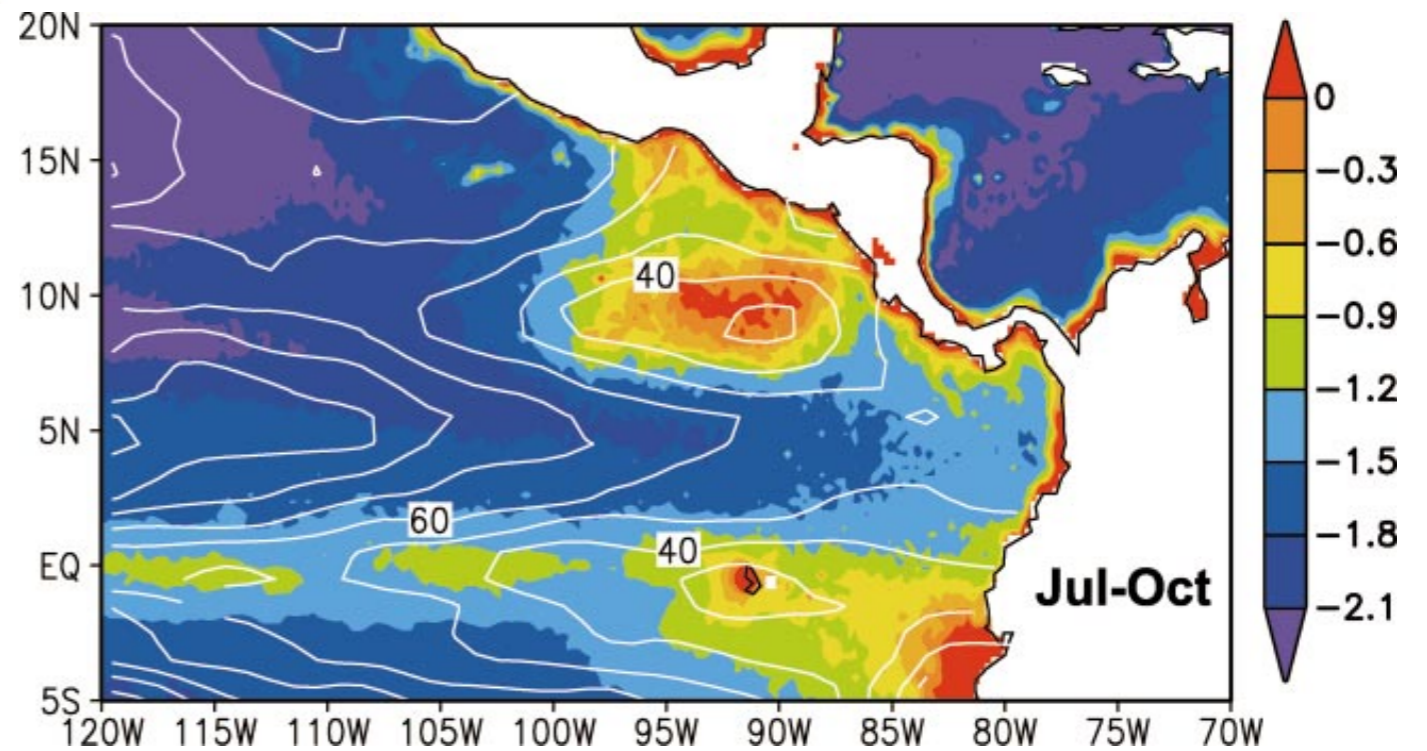
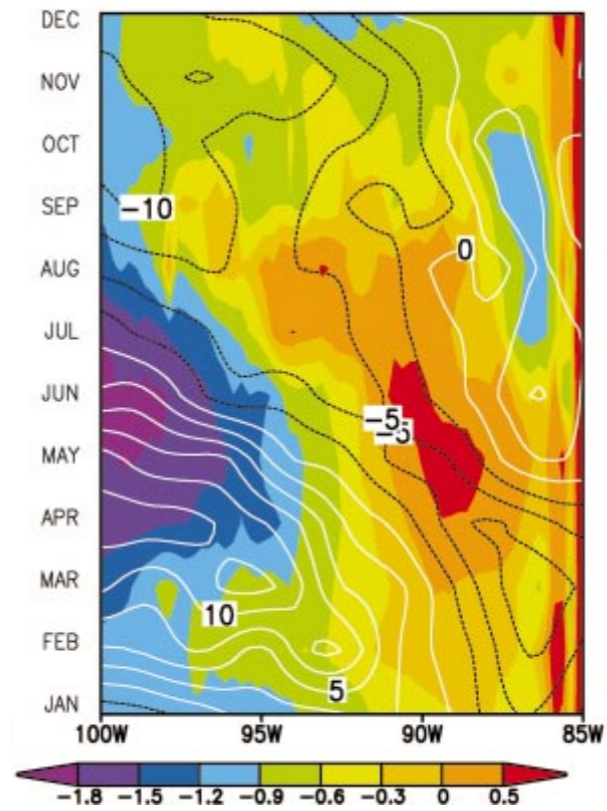


FIG. 7. SeaWiFS chlorophyll in natural logarithm (shade; $mg m^{-3}$) and $20^{\circ}C$ isothermal depth (contours; m) climatology for Jul-Oct.

Conclude

- Linear wind-driven dynamics explains much of the mean and annual cycle of the NETP: A region largely forced.
- Feedbacks to atmosphere primarily via persistent cold CRD.

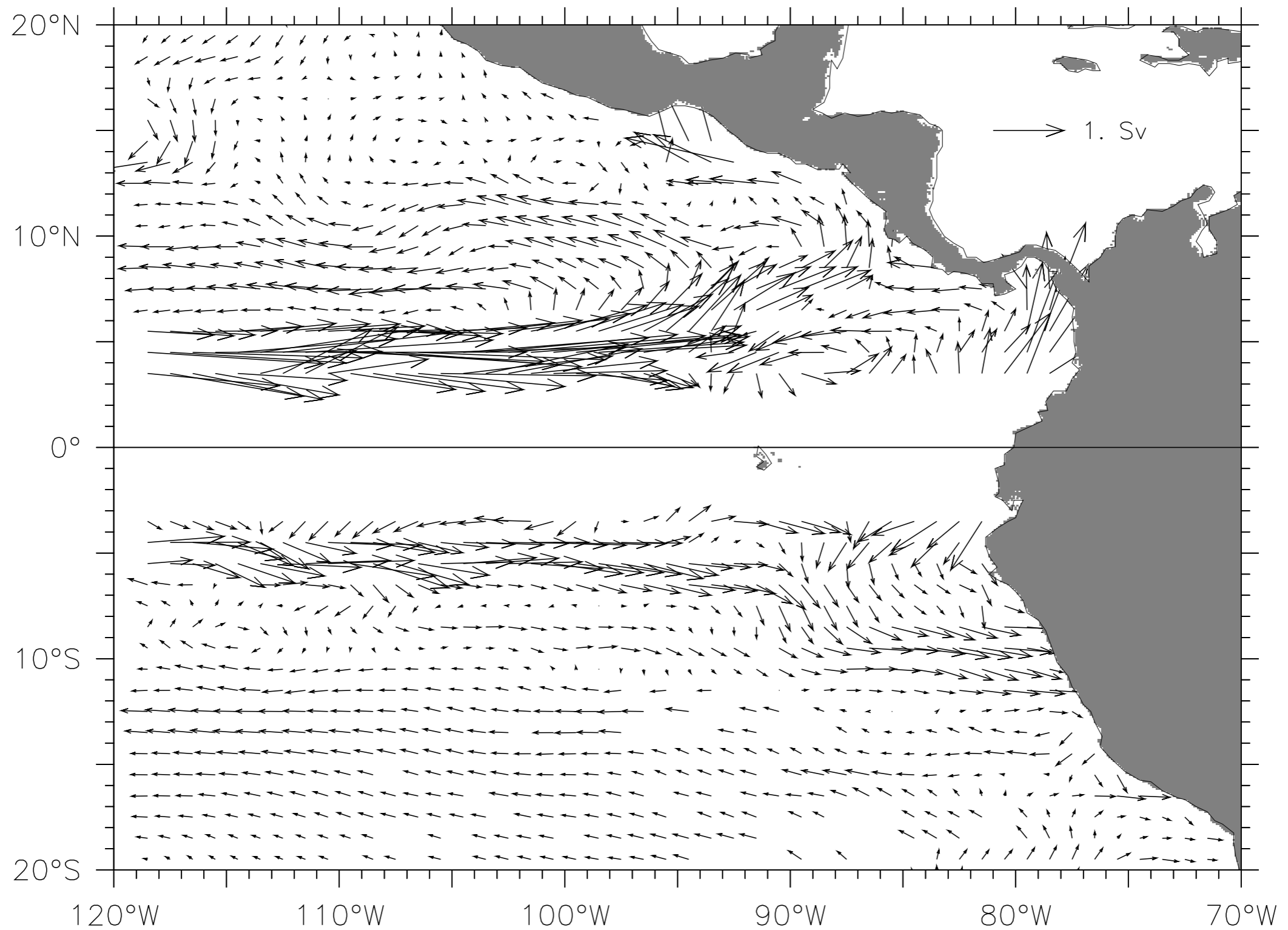
Open questions for research:

- Mechanisms for producing/sustaining anti-cyclonic eddies in summer (And is the Tehuantepec Bowl a real mean feature?)
- What determines the deep upwelling of the Costa Rica Dome? Why is it like Peru upwelling but unlike equatorial upwelling?
- How do the currents interconnect at the eastern boundary? (3-D)

Extras

Circulation below the thermocline

Transport between 450m and 17°C (XBT geostrophy)

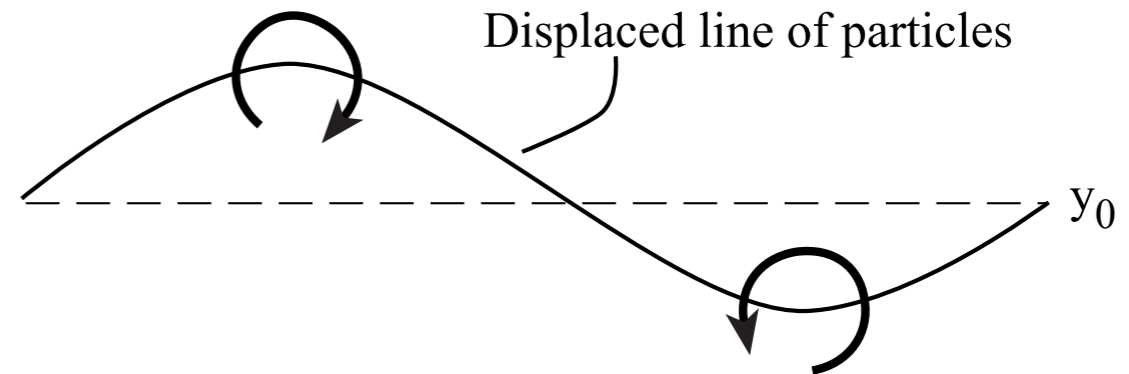


The mechanism of Rossby wave propagation

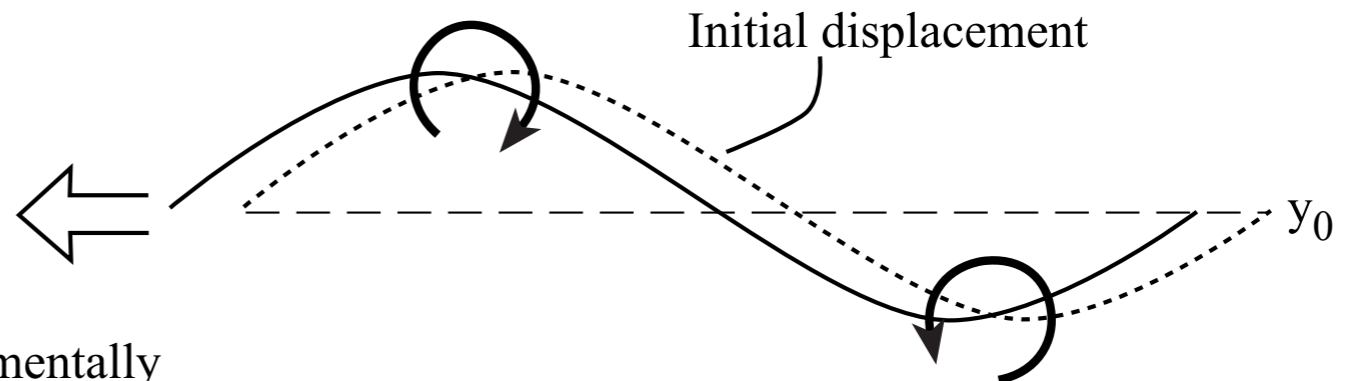
Consider a line of fluid particles, initially at rest along a line of latitude in the northern hemisphere:



The line is displaced meridionally by an external forcing (solid line). Conserving total vorticity ($\zeta+f$), particles displaced northward, where f is larger, acquire negative (clockwise) vorticity relative to surrounding water, while those displaced southward acquire positive relative vorticity :



The acquired relative velocities move the displaced line of particles to the west:



⇒ Rossby waves depend fundamentally on the variation of f with latitude.

Full derivation of Rossby waves

Consider the unforced ($\tau = 0$) “Fundamental” equations (1)-(3). Take the Curl of (1) and (2):

$$(v_x - u_y)_t + f(u_x + v_y) + \beta v = 0, \quad (1)$$

where $\beta \equiv df/dy$. Then take the divergence of (1) and (2):

$$(u_x + v_y)_t - f(v_x - u_y)_t + \beta u = 0. \quad (2)$$

Eliminate the relative vorticity $\zeta = (v_x - u_y)$ between these, and use (3) for the divergence ($u_x + v_y$):

$$\left(\frac{\partial^2}{\partial t^2} + f^2\right) h_t - \beta H(u_t + fv) = -g'H\nabla^2 h_t. \quad (3)$$

It is possible, though laborious, to derive an equation in h alone from (3), but easier to get an equation for v (Gill section 11.4). A simplification is to assume that v is geostrophic in the β term; this is equivalent to assuming that $u_t = 0$ in Fundamental equation (1). Thus:

$$\underbrace{\frac{1}{f^2} h_{ttt} - \frac{c^2}{f^2} \nabla^2 h_t}_{\text{gravity waves (no rotation)}} + \underbrace{h_t - \frac{\beta c^2}{f^2} h_x}_{\text{long Rossby waves}} = 0, \quad (4)$$

$\underbrace{\hspace{10em}}_{\text{all Rossby waves (low-frequency motion)}}$
 $\underbrace{\hspace{10em}}_{\text{Poincaré waves (long waves on } f\text{-plane)}}$

where $c \equiv \sqrt{g'H}$ is the gravity wave speed (in the reduced gravity model, $c \approx 2.5 \text{ m s}^{-1}$). If the wind stress terms in the Fundamental equations (1) and (2) are carried through this derivation, the simplifying assumption to get (4) is that v is geostrophic + Ekman (i.e. $u_t = 0$ as before). Then the forcing term on the right side of (4) would be:

$$-Curl\left(\frac{\tau}{f}\right) - \frac{1}{f^2} \frac{\partial}{\partial t} (\nabla \cdot \tau).$$

The dispersion relation for Rossby waves is found by omitting the high-frequency term h_{ttt} and assuming solutions to (4) proportional to $\exp\{i(kx + ly - \omega t)\}$, where (k, l) is the horizontal wavenumber and ω the frequency:

$$\omega = -\beta k / (k^2 + l^2 + f^2/c^2). \quad (5)$$

The length-scale $a_e = c/f$ is known as the “Rossby radius of deformation”. When the scale of the disturbance is larger than a_e (thus (k, l) is smaller than $1/a_e$), the $k^2 + l^2$ term in the denominator of (5) can be neglected. (Alternatively, $\nabla^2 h_t \ll \beta h_x$ in (4)). These are long Rossby waves (discussed on the next page), with the linear dispersion relation

$$\omega = -\beta k c^2 / f^2 \quad (6)$$